JET-P(95)08

Impurity Retention by Divertors Part 1: One-dimensional Models

P C Stangeby[1], J D Elder[1].

JET Joint Undertaking, Abingdon, Oxfordshire, OX14 3EA, UK.
[1] University of Toronto Institute for Aerospace Studies, Ontario, Canada, M3H 5T6.

Preprint of a paper to be submitted for publication in
Nuclear Fusion

April 1995

Abstract

An analytic Simple Fluid Theory, SFT, is derived to predict when a tokamak divertor should retain impurities. Only the simplest, one-dimensional case of leakage as *ions* from the point of ionization, along $\vec{B}$ to points far upstream is considered The SFT builds directly on earlier 1-D treatments of divertor retention of impurities. It is found essential to introduce cross-field leakage into the SFT, associated with the two-dimensionality of the actual divertor situation, otherwise the upstream regions suffer catastrophic — and unphysical — impurity accumulation. Without this correction, divertor leakage is predicted to occur even under rather cold (collisional) divertor operation. With this correction, leakage is predicted to occur only for divertor temperatures which are so high as to be unlikely of occurrence — at least for the case where impurity neutrals sputtered from the target plate are ionized on their first pass through the divertor plasma fan — the "shallow injection" case. Thus, previous analytic prescriptions for divertor retention are too pessimistic. For "deep injection" cases, as can occur with recycling gases such as neon, or with wall sputtered sources, a prescription is found for the plasma temperature above which impurity leakage occurs. The most critical factor governing retention is the location at which the impurity neutrals are first ionized. The predictions of the Simple Fluid Theory are compared with results using the Monte Carlo impurity transport code DIVIMP (Divertor Impurity). Close agreement is found for plasma conditions which are strongly collisional, but for weaker collisionality the SFT is found to overestimate leakage.

1. Introduction

The original motivation for employing a divertor, in magnetically-confined plasma devices, was to suppress the level of edge-produced impurity ions in the confined plasma. It seems plausible that if the location of the most intense plasma-surface interaction is made more remote from the confined plasma, then core contamination will be reduced for a given impurity production rate. This would certainly be true if the impurity particles were only transported from their release point to the confined plasma as *neutrals:* a limiter is, by definition, in intimate physical contact with the confined plasma since its inner tip defines the last closed surface; thus some of the neutral impurity particles sputtered, evaporated, etc., from the limiter tip always penetrate the confined plasma before being ionized. By removing the divertor targets some distance from the confined plasma it should be possible to prevent virtually all target-released neutrals from penetrating to the confined plasma before ionizing.

We must, however, also consider the possibility that the impurity will be transported as an *ion* from its point of ionization along the Scrape-Off Layer (SOL), flux tubes — to the periphery of the confined plasma, where by cross-field transport it will gain entry to the confined plasma. Even if the impurity can only travel a short distance as a neutral from the target before being ionized, it is possible that leakage as an ion may be very effective.

This aspect of divertor impurity behaviour is the focus of the present paper. It is only the first step in answering the larger question of whether a divertor can be expected to be an effective means of impurity control in a tokamak. In order to answer the larger question one also has to consider:

(a) the case of leakage which depends strongly on transport as a neutral, e.g., volatile impurities released at the target,

(b) wall-released impurities; these could be released by energetic charge-exchange neutral hydrogen bombardment of the walls or by chemical sputtering, etc.; the released material may

include, not just the original wall covering, but material from the targets which migrated by successive sputtering steps along the walls,

(c) the core-produced impurity, helium.

It is appropriate to make some comments on these last three processes by way of putting the present work in context. A number of experimental studies has been carried out on divertor retention of volatiles such as helium, neon and argon [1-6]. Unfortunately, there are a number of different routes by which impurities could reach the confined plasma in such cases, and it is not straightforward to assess the relative importance for each route: (a) the original puff location is generally not right at the target plate and the core contamination is probably strongly dependent on puff location, (b) some of these gases can be strongly recycling (and the recycle coefficient is not necessarily spatially or temporally constant), and the secondary source, associated with recycle at the targets, can quickly become much stronger than the primary (puff) source.

It is beyond the scope of the present work to consider the case of strongly recycling neutrals which cover a large part of the distance from the target to the core in the neutral state. That case will be dealt with separately. It is, however, within the present analysis to consider the final step of such a process, viz., starting at the point where the neutral is finally ionized — at some appreciable distance from the target. This will be termed the "deep injection" case.

In the present work the impurity ion is taken to be injected at a specified and arbitrary distance from the target, either shallow or deep.

A study, preliminary to the present work, has been presented previously [7].

2. Defining the "Simple One-Dimensional Case" for Modelling Impurity Retention by Divertors

We define the simplest possible case which will still contain the most basic elements of a divertor as they pertain to the retention/leakage of impurities:

(a) We start with the particle as an ion at some specified distance from the target and assume that the impurity ions can only move along $\vec{B}$. The definition of "leakage" is based either on the fraction of the injected ions which leak past a specified upstream point (corresponding to the target-to-X-point distance, for example), or on the ratio of impurity density far upstream to the density near the target. The background plasma, here taken as D^+/e, is assumed to flow toward the target at all points, or to be stagnant. Thus flow reversal of the background plasma is not allowed, although in reality such 2-D behaviour may be an important leakage mechanism [8]. The 1-D plasma background is taken as given or specified, and not directly altered by the impurities. Other assumptions of the model are:

(b) Impurity-impurity collisions are not included.

(c) Poloidal diamagnetic and $\vec{E}\times\vec{B}$ drifts are not included.

(d) Steady-state is assumed.

(e) The ionization state is taken to be frozen, typically as C^{4+} ions, with ionization/ recombination turned off.

(f) The impurity ion is taken to be everywhere in thermal equilibrium with the deuterons, $T_Z = T_D$.

Such a simple 1-D case has been treated by a number of authors [9-12] yielding a variety of more-or-less simple prescriptions to indicate under what circumstances the impurities would be expected to leak. The present work (Part I) is a re-visit of this simplest case which finds both elements of agreement with the earlier prescriptions as well as significant differences.

The approach consists of two principal components: the Simple Fluid Theory, SFT, and a Monte Carlo (numerical) code DIVIMP (Divertor Impurity) [13, 14]. Virtually all the physical processes normally used in DIVIMP are turned off in order to match the assumptions made for this simplest 1-D case.

One feature of DIVIMP which cannot be turned off is its automatic inclusion of the effect of variations in mean free paths. Fluid models implicitly assume strong collisionality/short mean free paths. Monte Carlo codes such as DIVIMP are quasi-kinetic in that all levels of collisionality are

automatically allowed for. Therefore, one of the purposes of using DIVIMP to test the predictions of the SFT is to identify the onset of collisionlessness and to see how leakage is changed compared with results for the collisional regime.

A further purpose in using DIVIMP is to study the effect of relaxing each of the simplifying assumptions listed earlier. This is impossible to do analytically. The use of a constrained DIVIMP in Part I introduces the first element of complicating effects, namely incomplete collisionality.

Although these Part I studies could be carried out in a simple 1-D geometry, in anticipation of Part II and the need to make direct comparisons at that time with the results of Part I, a standard 2-D spatial grid generated for JET has been used. The studies reported employed the first poloidal grid ring in the SOL for this particular mesh, which happened to have a plate-to-plate distance of 73 m (single null divertor configuration). It was useful to employ such a 2-D grid since this permitted the application of the 2-D hydrogenic neutral code NIMBUS [15] to the grid, with specified 2-D plasma background, in order to establish where the hydrogenic ionization occurred. Such information is needed to specify realistic hydrogenic ionization distributions when calculating the 1-D plasma background needed for the present study.

In the following Section the Simple Fluid Theory is developed and its results are compared and contrasted with earlier simple prescriptions. The earlier prescriptions took the near-target impurity density, here called n_p, to be given; here we will also develop prescriptions for this quantity, as well as for the leakage from this "base" or "plateau" (thus "p") level.

Perhaps the most important result from earlier prescriptions is that leakage will be small provided the plasma temperature in the divertor is sufficiently low, $\lesssim$ 20 eV [11]. We wish to re-assess this finding.

3. The Simple Fluid Theory, SFT: A 1-D Model of Impurity Leakage from a Divertor

3.1 The Momentum Equation

The force on the impurity ion is given by [16, 9]:

$$F_{total} = -\frac{1}{n}\frac{dp}{ds} + m\frac{(v_D - v)}{\tau_s} + ZeE + \alpha_e \frac{dT_e}{ds} + \beta_i \frac{dT_i}{ds} + \ldots \qquad (1)$$

where the lack of a subscript indicates the impurity; the first term is the impurity pressure gradient force per particle; the second term is due to friction with the background (D^+) plasma flow at specified velocity $v_D(s)$ and Spitzer stopping time τ_s; the third term is the electric force, specified, E(s); the fourth and fifth terms are the electron and ion temperature-gradient forces, with $T_e(s)$ and $T_D(s)$ specified; other forces, such as viscosity, are not considered here; s is measured along $\vec{B}$; s = 0 at target, s = L at the half-way point to the other target.

Consider first the case when (a) the only forces are the impurity pressure gradient force and the force of friction in a stagnant background plasma, i.e., $v_D = 0 = E = dT_e/ds = dT_i/ds$, and (b) collisionality is strong enough that the inertia mdv/dt can be neglected, i.e., $F_{total} = 0$, and (c) $T = T_D$, constant in space. One can then rearrange Eq. (1) to give:

$$\Gamma \equiv nv = -D_{\|}\, dn/ds \qquad (2)$$

where

$$D_{\|} \equiv \tau_s\, kT/m \equiv \tau_s\, v_{th}^2 \qquad (3)$$

It is thus seen that inclusion of the impurity pressure gradient force has the same effect on transport of particles as inclusion of parallel diffusion. This fact is used in Monte Carlo impurity transport

codes, including DIVIMP, Sec. 4, where the impurity pressure gradient force is not included explicitly, but rather parallel diffusion (in space or velocity) is used.

3.2 Region A: The Plateau or Prompt-Loss Region

For the case just considered, and assuming all the impurity ions are injected at location s_{inj}, then in steady-state the impurity density profile, n(s), will be the simple one shown in Fig. 1, with a "plateau" density:

$$n(s_{inj}) \equiv n_p \approx s_{inj}\, \phi_{in}/D_{\|} \tag{4}$$

where ϕ_{in} = injection rate of ions per sec per m^2 of area perpendicular to the plasma flow. A symmetry or reflection point is assumed to exist at $s = L > s_{inj}$. The result in Eq. (4) is approximate since the density just in front of the target, n(o), has been assumed to be negligible compared with n_p; in fact, $n(o) \approx \phi_{in}/v_{th}$ (v_{th} is the impurity thermal speed), but often $v_{th} >> v_{diff}$ where:

$$v_{diff} \equiv D_{\|}/s_{inj} \tag{5}$$

since $v_{diff} = v_{th}^2 \tau_s/s_{inj} = v_{th}\,(\lambda_{mfp}/s_{inj})$ where

$$\lambda_{mfp} \equiv v_{th}\tau_s \tag{6}$$

That is, when the mean free path for collisions between impurity and plasma ions $\lambda_{mfp} << s_{inj}$ one can neglect $n(o)/n(s_{inj})$. Since $\tau_s \propto T_D^{3/2}/n_D Z^2$, these assumptions give $D_{\|} \propto T^{5/2}$ and so $n_p \propto T^{-5/2}$. For this case $n_p = n_u$, the upstream density, i.e., the density adjacent to the core plasma — which directly gives the leakage to the core. Thus the leakage will actually *decrease* strongly with increasing T, which is the opposite to earlier expectations (and also, one should

emphasize, to the more typical case, as considered below). For the collisionless extreme, $\lambda_{mfp}/s_{inj} >> 1$, we expect that $n_p \approx \phi_{in}/v_{th}$, which gives a weaker, but still inverse temperature dependence, $n(L) \propto T^{-1/2}$.

Consider next the case where the force of friction, FF, dominates all other forces and also assume strong collisionality so that the acceleration (inertia) can be neglected. In this case one has $v = v_D$ and thus $n_p \approx \phi_{in}/v_D$.

When the ion-temperature force, FiG, is dominant, with strong collisionality and $v_D = 0$, then one has, from Eq. (1)

$$v \approx v_{T_i} \equiv \beta_i \tau_s (dT_i/ds)/m \tag{7}$$

One therefore expects for the general case:

$$n_p \approx \begin{cases} \phi_{in}/v_{th} & \text{for } \lambda_{mfp} >> s_{inj} \\ \phi_{in}/v_{prompt\,loss} & \text{for } \lambda_{mfp} << s_{inj} \end{cases} \tag{8}$$

where $$v_{prompt\,loss} \equiv v_{diff} + v_D + v_E - v_{T_i} - v_{T_e} \tag{9}$$

and $$v_E \equiv \tau_s ZeE/m \tag{10}$$

$$v_{T_e} \equiv \alpha_e \tau_s (dT_e/ds)/m \tag{11}$$

Equation (9) is directly derived from Eq. (1) by neglecting inertia, assuming T = constant, and approximating dn/ds by n/s_{inj}. The signs in Eq. (9) assume the usual situation where FF and the electric force, FE, are toward the target, while FiG and the electron-temperature gradient force,

FeG, are away from the target. Often |FF| > |FE| and |FiG| > |FeG| and so in the following FE and FeG are usually neglected for simplicity.

The existence of a density "plateau" extending from s_{inj} to L assumes $v_D \equiv dT_i/ds = 0$ in the region upstream of s_{inj}. If, in fact, |FF| < |FiG| in this latter region, then there will not be any density plateau, but rather the density will build up, causing catastrophic leakage to the core. Clearly, then, a necessary (but as will be shown, not sufficient) criterion for the avoidance of leakage is that |FF| > |FiG| in the region upstream of the injection point. This is the basis of the leakage criteria given by Neuhauser et al [9] and by Krashenninikov et al [10].

The Neuhauser criterion to avoid leakage is that:

$$M_D > \lambda_{DD}/\lambda_T \tag{12}$$

where $M_D \equiv$ Mach number of the deuterium plasma flow, $\lambda_{DD} \equiv$ the mean free path for collisions between deuterons and λ_T is the characteristic scale length for variations of T_i along s. One has $FF \approx M_D c_s m/\tau_s$, where $c_s \equiv$ deuterium plasma acoustic speed and $FiG = \beta_i T_i/\lambda_T \approx Z^2 T_i/\lambda_T$. With $\lambda_{DD} \approx c_s \tau_{DD}$ ($\bar{c}_i \approx c_s$ for $T_{D+} = T_e$) and $\tau_{DD}/\tau_s \approx m_D Z^2/m$ one then finds that requiring |FF| > |FiG| is the same as Eq. (12).

The Krashenninikov criterion to avoid leakage is that

$$q_i^{conv} > q_i^{cond} \tag{13}$$

where q_i^{conv}, q_i^{cond} are the ion power flux densities along s carried by convection and conduction. Neglecting the convected flow energy of $\frac{1}{2}$ mv^2nv, one has $q_i^{conv} = \frac{5}{2}$ $nvkT_i$ while $q_i^{cond} = \kappa_{io} T_i^{5/2}(dT_i/ds)$ where $\kappa_{io} \approx 60$ for T_i in [eV], dT_i/ds in [eV/m], q_i in [W/m^2] and $Z_{eff} = 1$. One can then readily show that requiring |FF| > |FiG| is the same as Eq. (13).

In the following we focus on the case where |FF| > |FiG| just upstream of $s = s_{inj}$ since it will turn out that even when this necessary condition is satisfied leakage may nevertheless occur. We

also note that since, generally, there is not a density plateau at $s = s_{inj}$, but rather a density peak (when $|FF| > |FiG|$) constituting a base level from which catastrophic leakage to the core sets in (when $|FF| < |FiG|$ upstream of $s = s_{inj}$). We will therefore call Region A, $0 \leq s \leq s_{inj}$, the "prompt loss region" and $n_p \equiv n(s_{inj})$ will refer to this "prompt loss" or near-target impurity density. The definition of *good divertor retention* or *low divertor leakage* then will be that $n_u/n_p << 1$, where n_u is the impurity density upstream, say at the X-point, where the SOL first comes into contact with the confined plasma. For the background plasma one often has $n_{Du}/n_{Dp} << 1$, due to $T_{Du}/T_{Dp} >> 1$ and pressure balance, but simple pressure balance does not apply to the impurity species.

3.3 Region B: The Impurity Density Decay Region

We consider n(s) profiles such as shown in Fig. 2, consisting of three regions:

1. Region A, the prompt-loss region, $0 \leq s \leq s_{inj}$, characterized by a density n_p typically near $s = s_{inj}$.
2. Region B is defined by $s_{inj} \leq s \leq s_v$, where $v_D \neq 0$ but $v_D \rightarrow 0$ at $s = s_v$. We assume that $|FF| > |FiG|$, hence that this is a region where n(s) decays. The characteristic scale length along s for v_D, i.e., the value of s_v, is given by the spatial distribution of the ionization of the deuterium neutrals recycling from the plate. To calculate this precisely requires sophisticated neutral codes such as DEGAS [17], EIRENE [18] or NIMBUS [15]. Vlases and Simonini [11], guided by NIMBUS code results for JET geometries, have provided the approximation:

$$s_v \approx 0.25/(n_e \times 10^{-20}) \text{ [m]} \qquad (14)$$

where n_e is the plasma density near the target. (Note that sv is measured along $\vec{B}$, and not in the poloidal direction.)

3. Region C where we will assume $v_D = 0$ and FiG is only opposed by (back-)diffusion in this impurity build-up region. Region C spans $s_v \leq s \leq L$.

The principal objective is to evaluate ϕ_{leak}, the one-way flux of impurities at s_v, and n_u/n_p.

Region B is a stagnant zone for impurities since it is upstream of both the source (at s_{inj}) and the sink (at s = 0), thus $v = F_{total} = 0$ here. Assuming $T = T_D = T_i$ one can then integrate Eq. (1) to obtain a result which is similar to ones found by Vlases and Simonini [11], Igitkhanov [19], Zagorski [20], and others:

$$n(s) = n_p \exp[FFf(s) + FEf(s) + FiGf(s) + FeGf(s)] \tag{15}$$

where the "f" refers to "factor" and:

$$FFf(s) \equiv \int_{s_{inj}}^{s} \frac{m v_D(s')ds'}{kT_i \tau_s} \tag{16}$$

$$FEf(s) \equiv \int_{s_{inj}}^{s} \frac{ZeE(s')ds'}{kT_i} = -\int_{V_{inj}}^{V} \frac{ZedV'}{kT_i} \tag{17}$$

$$FiGf(s) \equiv \int_{s_{inj}}^{s} \frac{(\beta_i - 1)(dT_i/ds')ds'}{kT_i}$$

$$= (\beta_i - 1)\, \ell n[T_i(s)/T_i(s_{inj})] \tag{18}$$

(the -1 in $(\beta_i - 1)$ comes from the T_i-dependence of the impurity pressure-gradient force).

$$FeGf(s) \equiv \int_{s_{inj}}^{s} \frac{\alpha_e(dT_e/ds')ds'}{kT_i} \tag{19}$$

Note that, usually, FFf(s), FEf(s) ≤ 0, while FiGf(s), FeGf(s) ≥ 0. Also for $s > s_v$ (Region C), FFf(s) = FFf(s_v) (and usually FEf(s) $\approx$ FEf(s_v)).

In cases where the variation of T_i is small over $s_{inj} \leq s \leq s_v$ one can ignore the variations of $T_i(s')$ and $\tau_s(s')$, making the evaluation of FFf(s) FEf(s), FeGf(s) much simpler. (Unfortunately, $kT_i\tau_s \propto T_i^{5/2}$ and for some cases, see Sec. 4.5, one has to allow for this variation in the integral, but this is straightforward. Since these factors appear in an exponential, small corrections to them can be important.) Let us take the case where this correction is unimportant and also assume $v_D(s) = v_{D_0} < 0$, a constant (out to s_v). Then for $s < s_v$:

$$FFf(s) \approx \frac{mv_{D_0}s}{kT_D\tau_s} \approx \frac{v_{D_0}}{D_{||}}\, s \equiv -\frac{s}{\lambda_{||}} \tag{20}$$

where we have also assumed s, $s_v >> s_{inj}$ and defined $\lambda_{||} \equiv -D_{||}/v_{D_0}$. Therefore if we ignore the other forces we find that n(s) decays with characteristic length $\lambda_{||}$, which is directly related to the prescription of Fussmann et al [1, 12] that to avoid leakage one needs a short $\lambda_{||}$, and thus low T (since $D_{||} \propto T^{1/2}$, then $\lambda_{||} \propto T^2$). Generally, however, one should include at least FiG, since β_i can be quite large, e.g., $\approx$ 32 for C^{4+} in D^+, and so even a weak T_i-gradient can influence the density decay length in Region B, λ_{decay}. Nevertheless, $\lambda_{||}$ gives a first estimate of λ_{decay}.

Thus an impurity density minimum occurs at s_v:

$$n(s_v) \approx n_p \exp[FFf(s_v) + FiGf(s_v)] \tag{21}$$

from which a build-up can then occur in Region C.

3.4 Region C: Impurity Density Build-Up or Trap Region

In Region C Eq. (15) applies again with $n(s_v)$ replacing n_p. One could combine Regions B and C, obviously, but there are good reasons not to do this, as discussed below.

Neglecting diffusion, leakage of impurities past point s_v is given by the particle flux density

$$\phi_{leak} = v_{T_i}\, n(s_v) \tag{22}$$

neglecting v_{T_e}; in equilibrium, diffusion gives an equal leakage back out of the trap located upstream of s_v, i.e., Region C. The density maximum in Region C generally occurs at s = L and can be of enormous magnitude since |FiGf(L)| can be much larger than |FFf(L)| = |FFf(s_v)|, and the difference in these factors appears in an exponential. *This result, fortunately, is an artificial and physically unrealistic one.* It is the consequence of assuming a strictly one-dimensional system, where the ions can only move along $\vec{B}$, i.e., along s. It can readily be shown that even very small cross-field losses will stop such an impurity build-up from occurring [21]. We may define the parallel de-trapping time (based on loss of the ions, by diffusion, from the trap region back past s_v in steady-state) by:

$$\tau_{||}^{\text{de-trap}} = \frac{N_{trap}}{A\phi_{leak}} \approx \frac{\bar{n}_t L}{\phi_{leak}} \tag{23}$$

where A = cross-sectional area of the SOL flux tube and $\bar{n}_t$ = average impurity density in the trap. This time can be >>1 sec. Consider, however, the effect of a competitive loss mechanism, say, cross-field transport into the Private Plasma or out to the periphery of the SOL, which will take $\tau_\perp \sim 10^{-3}$ to 10^{-2} sec (for $D_\perp \approx 1$ m^2/s and cross-field distances of cms). While there exists little understanding of how impurity ions behave in these peripheral regions of the edge plasma, these may be regions of weak collisionality and we will assume that ions which reach such flux tubes move along $\vec{B}$ to reach solid surfaces in impurity thermal transit times, i.e., ms. (Generally, it is found that the boundary conditions at the periphery of the SOL plasma are influential on the solutions — both for the background plasma and the impurities — and this remains an important, unresolved issue in the field of edge modelling.) A further possible de-trapping route, via

cross field transport, could be in the poloidal direction, back to the target, since only a short distance, $\approx (B_{pol}/B)\, s_{inj}$, may be involved [22]. Then $\tau_{de\text{-}trap}^{actual} = \left((\tau_{\parallel}^{de\text{-}trap})^{-1} + \tau_{\perp}^{-1} \right)^{-1}$ and so $\tau_{de\text{-}trap}^{actual} \approx \tau_{\perp}$. Thus, the actual value of $\bar{n}_t$ is:

$$\bar{n}_t = \phi_{leak}\, \tau_{\perp}/L = n(s_v) v_{T_i}\, \tau_{\perp}/L$$

$$= \frac{\phi_{in}}{v_{prompt\ loss}} \left(\frac{n(s_v)}{n_p} \right) v_{T_i} \frac{\tau_{\perp}}{L} \qquad (24)$$

where $v_{prompt\ loss}$ is given by Eq. (9), $n(s_v)/n_p$ is given by Eq. (21), v_{T_i} is given by Eq. (7). Thus, fortunately, $\bar{n}_t/n_p$ can be much less than unity, i.e., divertor retention of impurities can be much better than is indicated by a strictly 1-D analysis.

Although the original objective in this paper was to develop a <u>one</u>-dimensional model for impurity behaviour, we see that if we stick strictly to 1-D impurity transport the departure from reality can be enormous. One must, therefore, include at least this one particular 2-D effect, which, fortunately, requires only the foregoing simple correction.

It is thus seen that the larger the value of $D_{\perp}$ (i.e., the smaller the value of $\tau_{\perp}$), the *smaller* will be $\bar{n}_t$ and thus, in steady-state, the *smaller* the impurity content of the core plasma. This, possibly counter-intuitive conclusion, is strictly dependent on the assumption that the core impurity content does indeed reach steady-state equilibrium with the SOL upstream impurity density $\bar{n}_t$. In other circumstances, such as ELMing discharges where the core is periodically purged of impurities, there will be offsetting dependencies on $D_{\perp}$: large values of $D_{\perp}$ will, as before, carry impurities more effectively across the SOL into the (assumed) sink at the far periphery of the SOL, lowering $\bar{n}_t$; however, large values of $D_{\perp}$ will rapidly replenish the core impurity content between ELMs. The analysis of such time-dependent situations is not undertaken here, but will be examined in Part II.

3.5 Estimates of Divertor Leakage

3.5.1 General Formulation

In order to estimate ϕ_{leak} and $\bar{n}_t/n_p$, we need an estimate for dT_i/ds. For a first estimate, we base this on the value of dT/ds which would exist, at the target, if all the power flux density at the target were carried by electron parallel heat conduction and $T_e = T_i$:

$$\kappa_{oe} T_o^{5/2}(dT/ds)_o = \gamma_{sh} n_o c_{s_o} k T_o \tag{25}$$

Thus, $(dT/ds) \propto n_o/T_o$ ("o" for target conditions). Assume $v_{prompt\ loss} \propto T_o^{1/2}$ (the case $v_{prompt\ loss} = v_{th}$ or $v_D = c_s$, for example). We have $v_T \propto \tau_s T_o' \propto T_o^{1/2}$, independent of density. Taking $s_{inj} << s_v$ and assuming a small T-rise over $s_{inj} \leq s < s_v$ [which allows one to use the approximation $\ell n(1 + x) \approx x$, in evaluating $FiGf(s_v)$] one finds that ϕ_{leak} and $\bar{n}_t$ vary as $c_1 \exp(-c_2 n_o s_v/T_o^2)$ where c_1, c_2 are constants (or at least are independent of n_o, T_o, s_v). If, further, $s_v \propto n_o^{-1}$, Eq. (14), then ϕ_{leak} and $\bar{n}_t$ depend only on T_o, as $\exp(-c_3/T_o^2)$. These predictions of the Simple Fluid Theory are tested in Section 4.

As a next level of refining estimates, let us assume that the $T_i(s)$ profile is given by the modified heat conduction result:

$$\frac{T_i(s)}{T_i(o)} = \left[1 + \frac{7}{2} \frac{f_{cond} P s}{\kappa_{o_e} T_o^{7/2}}\right]^{2/7} \tag{26}$$

where P is the power flux density at the target and f_{cond} is the fraction of the power carried along the SOL by electron conduction. Inclusion of the factor $f_{cond} < 1$ thus allows for the effect of parallel heat convection (i.e., $f_{cond} < 1$). It is also a crude but convenient way to allow for other effects such as: (a) the fact that T_i does not necessarily equal T_e (this raises the effective $f_{cond} > 1$,

since in reality κ_o decreases if T_i is set by ion conduction), (b) inclusion of volume energy loss processes such as radiation, or effective volume energy loss processes in the divertor, such as cross-field heat flow into the Private Plasma, which also raises the effective $f_{cond} > 1$, i.e., makes dT/ds larger. We are therefore interested in values of f_{cond} centred at unity but spanning, possibly, from 0.1 to 10. Defining $\Delta s \equiv s_v - s_{inj}$ we therefore have:

$$FiGf(\Delta s) = (\beta_i - 1)\, f_{cond} P \Delta s / \kappa_o T_o^{7/2} \tag{27}$$

where the approximation $\ell n(1 + x) \approx x$ has been used. For FFf(s) we assume that the s-variations of $kT_i\tau_s$ in the integral equation (16) can be neglected, thus:

$$FFf(\Delta s) = -M_D c_s \Delta s / D_{||} \tag{28}$$

where M_D = Mach number of the deuterium plasma flow averaged over $s_{inj} < s < s_v$. We have

$$P = \gamma_{sh} n_o c_{s_o} k T_o \propto n_o T_o^{3/2}, \quad D_{||_o} = \hat{D}_{||_o} T_o^{5/2}/n_o, \quad c_{s_o} = \hat{c}_{s_o} T_o^{1/2} \tag{29}$$

where $\hat{D}_{||_o} = 3.55 \times 10^{18}$ m^2/s for T_o in [eV], n_o in [m^{-3}] and C^{4+} ions in a D^+ plasma, and $\hat{c}_{s_o} = 9788$ m/s for T_o in [eV] and D^+. We find that the same parameter grouping, $(n_o \Delta s/T_o^2)$, appears in both FiGf(Δs) and FFf(Δs). Thus $n(s_v)/n_p$ depends only on $(n_o \Delta s/T_o^2)$, f_{cond}, and M_D (and if $\Delta s \approx s_v$ and $s_v \propto n_o^{-1}$, then only on T_o, f_{cond}, and M_D). We will show shortly that often divertor retention will be good if $n(s_v)/n_p \leq 0.1$. We therefore define T_o^{th} as the threshold value of temperature in the divertor to achieve good impurity retention, and show from the foregoing that:

$$T_o^{th} = c(n_o \Delta s)^{1/2} \tag{30}$$

where

$$c \equiv [(c_a M_D - c_b f_{cond})/2.3]^{1/2} \tag{31}$$

and $$c_a \equiv \hat{c}_{s_0}/\hat{D}_{ll_0} \tag{32}$$

$$c_b \equiv \gamma_{sh}\hat{c}_{s_0}e/\kappa_0 \tag{33}$$

$e = 1.6\times10^{-19}$, $\kappa_0 \approx 2000$ for $Z_{eff} = 1$, $\gamma_{sh} = 7$, thus $c_a = 2.76\times10^{-15}$ and $c_b = 1.75\times10^{-16}$ for the example of C^{4+} in D^+ (where $\beta_i = 32.82$). n_o in [m^{-3}], Δs in [m], T in [eV].

We turn now to the claim that if $n(s_v)/n_p \leq 0.1$ then divertor retention will be good. Considering Eq. (24) one can evaluate v_{T_i} from Eq. (7), for T_o ranging from 10 - 100 eV, C^{4+} in D^+, $f_{cond} = 1$ to find that v_{T_i} only varies from ~2000 to ~6000 m/s. With $\tau_\perp \sim 10^{-2}$ s and L ~ 30 m one thus sees that $(v_T\tau_\perp/L) \approx 1$ (for C^{4+} in D^+). Thus $\bar{n}_t/n_p \approx n(s_v)/n_p$, i.e., there is little change in n(s) upstream of s_v (at least for this example of C^{4+} in D^+; for other combinations appropriate adjustments should be made). Thus we take $n(s_v)/n_p \leq 0.1$ as the criterion here for good divertor retention of C^{4+} in D^+.

3.5.2 Estimates of Hydrogenic and Impurity Ionization Lengths

As Eq. (30) makes evident, divertor retention of impurities depends predominantly on $\Delta s \equiv s_v - s_{inj}$, i.e., on achieving a region of significant hydrogenic flow velocity which extends as far as possible upstream of the point where the impurities are ionized. (It is generally not sufficient to merely have high flow velocity at the impurity ionization point.) Fortunately, even natural hydrogenic recycling tends to result in $s_v > s_{inj}$ for most impurities. For "deep injection" cases, e.g., recycling gases such as neon, special efforts may be required to increase s_v, such as strong hydrogenic pumping at the target region, combined with gas puffing far upstream.

For present purposes we only seek an estimate of s_v for natural recycling. Fortunately T_o^{th} depends only on the square root of Δs.

Hydrogenic neutral penetration into a plasma, allowing for the effect of charge exchange can be estimated [23-26] by:

$$\lambda_{pen}^{H} = \frac{(kT/m_H)^{1/2}}{n_e[\overline{\sigma v}_{iz}(\overline{\sigma v}_{iz} + \overline{\sigma v}_{cx})]^{1/2}} \tag{34}$$

The temperature dependence of λ_{pen}^{H} is rather weak, and for 10 eV $\leq$ T $\leq$ 1000 eV one has $\lambda_{pen}^{H} \approx (3\times10^{-19}\, n_e)^{-1}$ [m] to within a factor of two. This penetration distance is essentially in the poloidal plane, and so allowing for a magnetic pitch $B_\theta/B = 0.1$ one obtains the estimate:

$$s_v \approx \frac{0.3}{[10^{-20}\, n_e]} \quad [m] \tag{35}$$

which is very close to the estimate given by Vlases and Simonini, Eq. (14).

The foregoing neglects ionization of molecular hydrogen and so the NIMBUS code [15] was used to generate more realistic estimates, for the particular JET grid being used, and assuming a range of plasma conditions — various n_e, T, T_D+, although spatially constant. The value of s_v was taken here to be given by:

$$s_v = \int_o^L \Gamma_D(s)\, ds/\Gamma_D(0) \tag{36}$$

where $\Gamma_D(s)$ = deuterium ion flux density = $n_D(s)\, v_D(s)$, calculated along the separatrix flux tube, using the ionization source directly from NIMBUS. The results are shown in Table I.

Table I

n_e [m^{-3}]	T_e [eV]	T_i [eV]	s_v [m]
10^{19}	10	10	3.0
10^{19}	100	10	0.93
10^{19}	10	100	2.3
10^{19}	100	100	1.1
10^{20}	10	10	0.061
10^{20}	100	10	0.026
10^{20}	10	100	0.22
10^{20}	100	100	0.049

As can be seen, the approximations of Eqs. (14) or (35) are within a factor of 2 for $n_e = 10^{19}$ m^{-3} but are somewhat high for $n_e = 10^{20}$ m^{-3}. We will therefore take Eq. (14) only as a guide for estimating s_v in the present study.

Turning next to the impurities, we will take carbon physically sputtered by D^+ as an example. Suppose the energy of the sputtered carbon is ≈10 eV, thus $v_c \approx 10^4$ m/s. Suppose the plasma background is $T_e = 50$ eV, $n_e = 10^{19}$ m^{-3}, then the (poloidal) ionization distance is ~1 cm, and so $s_{inj} \approx 0.1$ m. The DIVIMP code was used to refine this estimate, for the same JET grid as before and with $T_e = T_{D^+} = 50$ eV, $n_e = 10^{19}$ m^{-3} constant in space. The sputtering data of [27] was used, together with the assumption of a cut-off Thompson energy distribution and a cosine angular distribution for the sputtered carbon [28]. The average sputtered energy was calculated to be 12.5 eV and the average $\bar{s}_{inj}$ was found to be 0.11 m, in close agreement with the simple estimate. A spatially varying plasma background was also used, with T decreasing from 50 eV on the separatrix to 14 eV at 4 cm out in the SOL (at the target), and n_e decreasing from 10^{19} m^{-3} to 10^{18} m^{-3}. The average carbon energy was calculated to be 9.9 eV and the value of $\bar{s}_{inj} = 0.24$ m, averaged over all the SOL flux tubes. It thus appears that simple estimates for s_{inj} will be adequate for the present study. One should note that neutrals released by self-sputtering will be somewhat more penetrating.

We can therefore conclude that for physically sputtered impurities, such as carbon (and even more so for heavier elements), s_{inj} is small compared with s_v. For chemically sputtered carbon, or evaporated atoms, then $s_{inj} << s_v$. (Backscattered helium, on the other hand, can have $s_{inj} \gtrsim s_v$; consider the example of a 50 eV He^0 entering a plasma with $T_e = 50$ eV, $n_e = 10^{19}$ m^{-3}, giving a (poloidal) ionization distance of ~0.3 m, thus s_{inj} perhaps 10× larger, which is comparable to s_v.)

3.5.3 Implications for Divertor Leakage

We return now to Eq. (30) to discuss its implications. As a reference case we will take $M_D = f_{cond} = 1$, thus $c = 3.35 \times 10^{-8}$ and so, for example, if $n_o = 10^{19}$ m^{-3} and $\Delta s = 1$ m , then $T_o^{th} = 106$ eV. One may note that this is a rather high temperature for the onset of divertor leakage compared with earlier thinking, see, e.g., [11]; the difference is a direct consequence of the use of $\tau_\perp$ rather than $\tau_\parallel$ in Eq. (24). Neutrals sputtered from the target are likely to be ionized at $s_{inj} < s_v$ and so most of Region B is a region where the deuterium flow velocity is significant, $M_D \approx 1$ and therefore convection is also strong. The latter effect, by itself, would make $f_{cond} < 1$; of course, incomplete equipartition and volume energy losses in the divertor could offset this reduction in f_{cond}. (Actually, for C^{4+} in D^+, where $c_a >> c_b$, the precise value of f_{cond} does not matter very much when $M_D \approx 1$, since $|FF| >> |FiG|$, and $\lambda_{decay} \approx \lambda_\parallel$, Eq. (20). So, for the parameter set $(M_D, f_{cond}) = (1, 0.1)$, one calculates $c = 3.45 \times 10^{-8}$ which gives $T_o^{th} = 109$ eV for $n_o = 10^{19}$ m^{-3} and $\Delta s = 1$ m. For the parameter set $(M_D, f_{cond}) = (1, 10)$, one calculates $c = 2.10 \times 10^{-8}$ which gives $T_o^{th} = 66$ eV for $n_o = 10^{19}$ m^{-3} and $\Delta s = 1$ m. These are not large changes from the result for the parameter set $(M_D, f_{cond}) = (1, 1)$ which gives $T_o^{th} = 106$ eV.) If we take $\Delta s \approx s_v$ and s_v from Eq. (14), then $T_o^{th} = 168$ eV, independent of density. Since these temperatures are rather high for a divertor, they indicate that *impurities sputtered from the target would be unlikely to ever leak to the main plasma* — by the direct, purely ion-transport route.

Of course, not all impurities released at the target will be ionized at $s_{inj} << s_v$. Backscattered helium, for example, can penetrate to s_v and beyond before ionizing. Consider, therefore, $\Delta s \rightarrow 0$; then $T_o^{th} \rightarrow 0$, i.e., the divertor leaks at all temperatures. In principle, all intermediate situations are possible, and so one cannot say that there is a unique value of T_o^{th} below which leakage does not occur, in fact $T_o^{th} \propto (s_v - s_{inj})^{1/2}$.

Consider now the deep injection cases, e.g., impurities which are injected as a result of wall sputtering and recycling gases such as He, Ne. While some of these neutrals, recycling from the target will be ionized near the target and (possibly) at $s_{inj} << s_v$, some will escape from the

One can also rewrite from Spitzer:

$$\left(\langle \Delta w_{\|})^2 \right\rangle \Delta t\right)^{1/2} = \left(\frac{kT_I}{m_I}\right)^{1/2} \left(\frac{2\Delta t}{\tau_{\|}}\right)^{1/2} \tag{40}$$

where

$$\tau_{\|} \equiv \frac{m_I T_I (T_D/m_D)^{1/2}}{6.8\times10^4\, n_D Z_I^{\,2}\, \ell n\, \Lambda} \tag{41}$$

in the same convenient units as Eq. (39).

The choice of the value of the calculational time step in DIVIMP, Δt, is specifiable and is usually chosen to be much smaller than the smallest value of τ_S, $\tau_{\|}$ for any charge state. The values of the plasma background quantities, E, v_D, dT_e/ds, dT_D/ds are specified by separate models either internal to the DIVIMP code ("SOL Options") or through direct coupling to 2-D edge fluid codes, such as EDGE 2D/NIMBUS [30] or B2/EIRENE [31]. Particularly simple SOL Options are used for the present work, see below.

Further details on the treatment of collisions are given in the Appendix.

The effect of finite values of $\tau_\perp$ was achieved in the present DIVIMP runs, not by actually using $D_\perp \neq 0$ and the full 2-D grid — which will be the method used in Part II — but simply by "killing off" the ions in a Monte Carlo way; at each time step Δt the ion was removed from the plasma if a random number x, uniform on [0, 1] fell within $0 < x < \Delta t/\tau_\perp$, where $\tau_\perp$ was specified (and was always chosen > Δt). Thus the cross-field loss time was taken as being constant, independent of s.

4.2 The Near-Target Impurity Density n_p

We consider first examples of code results to compare with the SFT value of n_p, Eq. (8). Figure 3 shows DIVIMP and SFT results for Case A (parameters for the different cases are summarized in Table II): T_{i_0} = 10 eV, dT_i/ds = 1.38 eV/m (constant), $n_e = 10^{19}$ m^{-3} (constant),

injection of ions uniformly within s_{inj} = [0.1 m, 0.2 m], various values of v_D in the range [-1500, -750 m/s], s_v = 1.2 m. Consider the example of v_D = -750 m/s for illustration: $\tau_{s_0} = 1.41\times10^{-6}$ s, thus $D_{ll_0} = kT_{i_0}\tau_{s_0}/m_I$ = 113 m^2/s and $v_{drift} = D_{ll_0}/\bar{s}_{inj}$ = 753 m/s; v_{T_i} = 510 m/s. The basic calculations in DIVIMP are here normalized to 10^{20} impurity ions per sec injected into "the system". Here, "the system" is a particular flux tube for the particular JET grid giving $\phi_{in} = 1.73\times10^{23}$ m^{-2} s^{-1}, a physically plausible level. Since the focus of the present paper is on the *efficiency* with which impurities contaminate the core plasma, the value of ϕ_{in} is unimportant. In our example we have: $v_{prompt\ loss}$ = 753 + 750 - 510 = 993 m/s and so one expects from the SFT that $n_p = \phi_{in}/v_{prompt\ loss} = 1.74\times10^{20}$ m^{-3}. As can be seen, the agreement is quite good for this highly collisional case, $\lambda_{mfp} \approx 0.01$ m. Figure 4 shows DIVIMP and SFT results for Case B: $n_e = 10^{20}$ m^{-3}, s_{inj} uniform within [0.1, 0.2 m], s_v = 1.2 m, M_D = 0.1, f_{cond} = 0.1 (as per Sec. 3.5 and Eq. (26)), various values of T_{i_0} as shown. At low T_{i_0}, where $\lambda_{mfp} << \bar{s}_{inj}$, the DIVIMP results approach the SFT result for high collisionality, ϕ_{in}/v_{pl}, while for high T_{i_0} the DIVIMP results start to approach the simple collisionless prediction, ϕ_{in}/v_{th}; note that at T_{i_0} = 110 eV, $\lambda_{mfp} \approx \bar{s}_{inj}$.

It therefore appears that the simple prescription given by Eq. (8) will give the value of the near-target impurity density to within a factor of 2. No better agreement can be expected since the SFT neglects inertia, and there has been no attempt to construct a transitional model to cover the collisional-collisionless transition.

4.3 The Density Decay Region

We consider next Region B, Fig. 2, the impurity density decay region and start with a simple test: only the electric-field force was turned on, with $v_D = dT_i/ds = 0$; T_i = 50 eV, E = -25 V/m, and $n_e = 10^{18}$, 10^{19} or 10^{20} m^{-3} (Case C). Thus one expects to find a density decaying according to the Boltzmann factor $\exp\left(-\frac{ZeEs}{kT_i}\right) = \exp(-s/\lambda_{BF})$ where $\lambda_{BF} \equiv kT_i/ZeE$ = 0.5 m. Results in Fig. 5 show excellent agreement for this case over about 6 orders of magnitude and for varying

degrees of collisionality: $\lambda_{mfp} \approx 3$ m for $n_e = 10^{18}$ m^{-3} and $\lambda_{mfp} \sim 0.03$ m for $n_e = 10^{20}$ m^{-3}. In a second basic test, $E = dT_i/ds = 0$ and $v_D = -112.2$ m/s, $n_e = 10^{19}$ m^{-3}, $T_i = 10$ eV (Case D). This gives $D_{||} = (kT_i/m_i)\,\tau = 112.2$ m^2/s and so one expects to find the SFT result, $n \propto \exp(-x/\lambda_{||}^{SFT})$ with $\lambda_{||}^{SFT} \equiv D_{||}/v_D = 1$ m, for this strongly collisional case, $\lambda_{mfp} = 0.01$ m. Results in Fig. 6 show that there is excellent agreement between the DIVIMP results and SFT for this case. Also shown in this figure are results with T_i raised to 100 eV and $|v_D|$ increased to $v_D = -3.55\times10^5$ m/s for $n_e = 10^{18}$ m^{-3} and to $v_D = -3.55\times10^4$ m/s for $n_e = 10^{19}$ m^{-3} (which keeps $\lambda_{||}^{SFT} = 1$ m), that is, two much less collisional cases ($\lambda_{mfp} \approx 10$ m and ≈ 1 m). Nevertheless, agreement with the SFT is still excellent. This possibly surprising result is discussed next.

Although one might expect that the density decay would only follow $\exp(-x/\lambda_{||}^{SFT})$ for highly collisional situations, in fact this variation is followed fairly closely even as $\lambda_{mfp}/\lambda_{||}^{SFT} \rightarrow \infty$. The reason for this is as follows. The momentum equation can be integrated to give the distance x_t, that the ion will travel upstream against the D^+ flow before being stopped and turned around by friction:

$$x_t = \tau_s \left[v_D \, \ell n \left[1 - \frac{v_o}{\langle v_o \rangle} \frac{\langle v_o \rangle}{v_D} \right] + \frac{v_o}{\langle v_o \rangle} \langle v_o \rangle \right] \qquad (42)$$

where v_o is the individual ion velocity at $t = 0$ when all the ions are launched from $x = 0$, and $\langle v_o \rangle$ is the average over the distribution of launch velocities. One notes that Eq. (42) holds for *all* levels of collisionality, however weak. Define

$$v_r \equiv v_o/\langle v_o \rangle, \quad \lambda_{mfp} \equiv \langle v_o \rangle \tau_s, \quad \langle v_o \rangle = \left(\frac{kT}{m}\right)^{1/2}$$

$$D_{||} \equiv \frac{kT}{m} \tau_s \qquad (43)$$

then:
$$x_t = \lambda_{mfp}\left[v_r - \frac{\lambda_{mfp}}{\lambda_{||}}\,\ell n\,\left[1 + v_r\,\frac{\lambda_{||}}{\lambda_{mfp}}\right]\right] \tag{44}$$

As $\lambda_{mfp}/\lambda_{||} \rightarrow \infty$ this gives

$$x_t \rightarrow \frac{\lambda_{||}}{2} v_r^2 \tag{45}$$

Since the number of ions with velocity v is proportional to $\exp(-mv^2/2kT)$ therefore the number of ions reaching x_t is proportional to $\exp(-x/\lambda_{||})$, the same result as for the highly collisional case. It is thus seen to be a basic physical fact that for the simple case of pure decay of density (where diffusion opposes frictional drag), the density profile is independent of the degree of collisionality.

4.4 Leakage from the Divertor. Shallow Injection

Figures 5 and 6 show a simple monotonic decay of density upstream of s_{inj} since the T_i-gradient force was absent. There will also be no leakage from the divertor for such cases. As the next step, FiG was turned on and v_D was assigned a non-zero value, thus giving the simplest approximation to the real situation in a divertor; the inclusion of FE and FeG does not change the essential nature of the problem and so for simplicity these forces are not included in the following.

Examples of n(s) are given in Fig. 7 for Case B, defined earlier, and the specific example of T_{i_o} = 100 eV, various values of $\tau_\perp$. Here $D_{||_o} = 3.6\times10^3$ m^2/s, $v_{T_i} = 640$ m/s, $v_D = -9.8\times10^3$ m/s, $v_{th} = 2.8\times10^4$ m/s, $\lambda_{mfp} = 0.13$ m and since $\lambda_{mfp} \approx \bar{s}_{inj} = 0.15$ m, one can estimate n_p from $\phi_{in}/v_{th} = 6.2\times10^{18}$ m^{-3}. As can be seen from Fig. 7, this agrees to within a factor of 2 of the value from DIVIMP. One also has $FFf(s_v = 1.2\text{ m}) = -2.75$, $FiGf(s_v) = +0.17$, thus one expects $n(s_v)/n_p = \exp(0.17 - 2.75) = 0.076$, which one can also see is approximately the value found by DIVIMP, Fig. 7. We also have $\phi_{leak}^{SFT} = v_{T_i} n(s_v) = 3.0\times10^{20}$ m^{-3}, so $\phi_{leak}^{SFT}/\phi_{in} = 1.7\times10^{-3}$. This

"plasma fan" and bounce off the walls to re-enter the plasma upstream and be ionized, perhaps near s_v or above it. If entry is above s_v then obviously core leakage could be extremely high (neglecting for the moment such inherently 2-D effects as cross-field transport and flow reversal). Even for impurity entry below s_v, M_D might be rather small, which would then mean that convection would be small and so $f_{cond} \approx 1$. We might then be dealing with a case with, for example, $M_D = 0.1$ and $f_{cond} = 1$, giving $c = 6.64 \times 10^{-9}$ and $T_o^{th} = 72$ eV for C^{4+} in D^+, $n_o = 10^{19}$ and $\Delta s = 10$ m (e.g., $M_D \approx 0.1$ over distance $\Delta s \approx 10$ m). Also, in this situation all values of Δs will arise and as $\Delta s \rightarrow 0$, again $T_o^{th} \rightarrow 0$, for example, for C^{4+} in D^+, $n_o = 10^{19}$ m^{-3} and $\Delta s = 1$ m, $T_o^{th} = 23$ eV. One sees that there is no unique temperature threshold below which divertor retention is good for deep injection cases. For shallow injection, e.g., sputtered carbon, however, it seems unlikely that divertor temperatures would ever be high enough to permit direct ion leakage (in the absence of flow reversal) — as already noted.

4. DIVIMP Code Tests

4.1 Brief Description of DIVIMP

DIVIMP [13, 14] is a Monte Carlo code which follows impurity neutrals and ions (only ions in the present study) in their 2-D motion along and across magnetic field lines in a specified plasma background (2-D distribution of T_e, T_{D+}, n_e, v_{D+}, E) allowing for (a) classical parallel motion, (b) anomalous cross-field motion with $D_\perp$ specified, (c) ionization/recombination change of state, and (d) finite thermalization of the impurity ion relative to the local T_{D+}. The impurity pressure gradient force is incorporated via parallel diffusion in DIVIMP, using either spatial or velocity steps. In order to have the most direct comparison with the fluid model predictions of the last section the following were implemented in the code: (a) ions injected as helium-like, i.e., C^{4+}, ions in a narrow s-band, with T = local T_{D+}, and thereafter the thermalization time was set to zero, ensuring that the impurity temperature always equalled the local T_{D+},

(b) ionization/recombination was stopped, (c) cross-field transport was stopped, (d) only FF and FiG (plus diffusion) were included.

The motion of the impurity ion along $\vec{B}$ is assumed to be classical and thus for the above conditions is described by:

$$\Delta v = \langle \Delta w_{\|} \rangle \, \Delta t + \left(\langle (\Delta w_{\|})^2 \rangle \, \Delta t \right)^{1/2} r_G + \frac{Z_I e E}{m_I} \Delta t$$

$$+ \frac{\alpha_e}{m_I} (dT_e/ds) \, \Delta t + \frac{\beta_i}{m_I} (dT_D/ds) \, \Delta t \qquad (37)$$

where $\langle \Delta w_{\|} \rangle$ and $\langle (\Delta w_{\|})^2 \rangle$ are the Spitzer collision coefficients [29], and r_G is a random number of Gaussian distribution with $\langle r_G^2 \rangle = 1$. The prescription for β_i in [9] is used here. Here $\alpha_e = E = 0$ is assumed. Allowing for the drift velocity of the background deuterium plasma along the SOL at velocity v_D, we can write:

$$\langle \Delta w_{\|} \rangle = (v_D - v)/\tau_S \qquad (38)$$

where the value of τ_S used here is extracted with the aid of Spitzer's Table 5.2 [29]; for simplicity we use Spitzer's tabulated value for $x \equiv$ "$\ell_f w$" $\equiv v/(2kT_D/m_D)^{1/2} << 1$; this gives:

$$\tau_S = \frac{m_I T_D (T_D/m_D)^{1/2}}{6.8 \times 10^4 (1 + m_D/m_I) \, n_D Z_I^2 \, \ell n \, \Lambda} \qquad (39)$$

where in Eq. (39) quantities are in the convenient units: τ in [s], T in [eV], m in [amu], n_D in [10^{18} m^{-3}]. We take $\ell n \, \Lambda = 15$, fixed.

value agrees well with the value found by DIVIMP, see Fig. 8 where a plot with other values of T_{i_o}, Case B, are also included.

One may note that Fig. 8 has been plotted vs. $T_{i_o}^{-2}$, in order to test the SFT prediction of Sec. 3.5 that $\phi_{leak} \propto \exp(-T_o^{-2})$, and, as can be seen, the DIVIMP results agree both with this trend, as well as the absolute magnitude predicted by the SFT — at least for this highly collisional case, $\lambda_{mfp} << s_v$.

Returning to the density profile plot, Fig. 7, we may compare the values of $n(s > s_v)$ with the predicted estimate of $\bar{n}_t^{SFT}$, Eq. (24), $\bar{n}_t^{SFT} = \phi_{leak}^{SFT}\tau_\perp/L$ with $\phi_{leak}^{SFT} = 3\times10^{20}$ m^{-2} s^{-1}, L ≈ 30 m, thus $\bar{n}_t^{SFT} = 10^{19}\,\tau_\perp$: for $\tau_\perp$ = 1, 10, 100, 1000 ms one thus has $\bar{n}_t^{SFT} = 10^{16}$, 10^{17}, 10^{18}, 10^{19} m^{-3}. As can be seen from Fig. 7, the DIVIMP profiles do give such average densities in the trap, approximately. Evidently $\tau_{||}^{de\text{-}trap} \approx 10$ sec for this example, as can be inferred from the fact that the n(s) profile is only a little higher for $\tau_\perp$ = 10 s than for 1 s. Indeed, the value of n(L) for $\tau_\perp = \infty$ is readily calculated (from FiGf(L), FFf(L)) and gives the value shown on Fig. 7 as a point — confirming that $\tau_{||}^{de\text{-}trap} \approx 10$ s.

The example of $\tau_\perp$ = 1 ms, Fig. 7, is noteworthy. While $\bar{n}_t^{SFT}$ does still give the trap content reasonably accurately, the actual leakage to the core plasma would not be proportional to $\bar{n}_t$ in this case, but to a substantially smaller value — namely the average value of n for $s \gtrsim s_{x\text{-}point}$, here about 8 m. This is due to the fact that the parallel transit time for impurity ions to travel from the divertor "confined" region at $s \lesssim s_v$ = 1.2 m, to the x-point exceeds $\tau_\perp$. Thus ions are lost (to the periphery) before they can reach the part of the SOL which is adjacent to the confined plasma. If achievable, this would be a most attractive state of affairs, clearly, since then there is no need to have a density decay region at all, i.e., *one would not need to have any friction force dragging the impurity ions to the target,* so even ions which enter the plasma above $s = s_v$ will not leak to the core. Such very short cross-field sink times, however, may not occur. This possibility, nevertheless, should not be lost sight of. It again brings out the importance of understanding what happens to impurity ions which reach the far periphery of the SOL and Private Plasma: are they promptly removed from the plasma or not?

We turn next to a less collisional example, only slightly different than Case B. Case E: $n_e = 10^{19}$ m^{-3}, $M_D = f_{cond} = 1$, $s_v = 1.2$ m, s_{inj} uniform within [0.1, 0.2 m], various values of T_{i_o} — a physically more likely case than Case B. Now one has $\lambda_{mfp} \sim 1$ m, comparable to s_v, and one might anticipate the onset of collisionless effects on ϕ_{leak}. Results for ϕ_{leak} are shown in Fig. 9, again plotted vs. $T_{i_o}^{-2}$. Although the DIVIMP results follow the trend predicted by the SFT, the absolute values of ϕ_{leak}/ϕ_{in} now fall significantly below the SFT predictions. This is due, in fact, to an effect of collisionlessness: since $\lambda_{mfp} \approx s_v$, the effect of FF does not abruptly stop at $s = s_v$. Rather its influence is felt further upstream by some distance of order λ_{mfp}. (There would be a similar, and at least partially offsetting effect if FiG existed only above $s = s_v$, but that is not the case.)

This particular consequence of decreasing collisionality, i.e., to *decrease* leakage, is contrary to the general underlying pattern, namely that decreasing collisionality *increases* leakage [in Sec. 3.5.1 recall that it was predicted that $\phi_{leak} \propto \exp(-cn_o/T_o^2)$, i.e., $\propto \exp(-c/\lambda_{mfp})$]. This only results, however, in a partial offset from the underlying trend. A qualitatively similar result was found by Krasheninnikov et al, Fig. 3 of Ref. [10], for a somewhat different case.

Closely related to these considerations is the matter of correcting the thermal gradient coefficients, α_e, β_i for the onset of collisionlessness. For typical ITER conditions, Krasheninnikov et al [10] estimated from kinetic analysis for He-ions in a DT plasma, that the value of β_i should be reduced by a factor of at least 2 or 3. Such changes have not been made here, but their effect would clearly be to reduce still further the impurity leakage from the divertor, compared with the SFT result.

The n(s) profiles for Case E are shown in Figs. 10a, b, c for $\tau_\perp = 1$, 10, 1000 ms. From Sec. 3 we have the SFT prediction for this case that leakage will be significant for $T_{i_o} > T_o^{th} = 106$ eV, i.e., that $n(s_v)/n_p \geq 0.1$ for $T_{i_o} > 106$ eV. One may observe from the plots that $n(s_v)/n_p \gtrsim 0.1$ for $T_{i_o} > 130$ eV. That is, the threshold for divertor leakage, as defined in Sec. 3, is approximately as predicted by SFT, although somewhat delayed to higher temperature. This delay is due to the partial collisionality of this case, as already discussed.

The value of n(L) for $\tau_\perp$ = 1000 ms in Fig. 10c is unrealistically high, approximately the unphysical characteristic of a strictly one-dimensional system referred to in Sec. 3. Results for the more realistic value of $\tau_\perp$, 10 ms, Fig. 10b shows that for T_{i_0} = 130 eV, the leakage is indeed marginal: for $\tau_\perp$ =10 ms, $\bar{n}_t/n_p \approx 0.1$, while for $\tau_\perp$ = 1 ms it is substantially less. One may note that the faster diffusion for Case E, compared with Case B, allows ions to travel as far as s = L before being "killed off" even for $\tau_\perp$ = 1 ms.

4.5 Leakage from the Divertor. Deep Injection

For the case of recycling gases, such as neon, a more important leakage route than the one of prompt ionization plus ion transport upstream against the deuterium flow, e.g., Case E, would be via neutrals which initially escape the divertor plasma fan, strike a side wall and then re-enter the plasma further upstream where $M_D << 1$. This is probably the situation in the impurity retention studies carried out by Janeschitz, Fussmann, Roth, Krieger, McCracken, et al [1-6]. We therefore consider the example Case F: $M_D = 0.1$, $f_{cond} = 1$, $n_e = 10^{19}$ m^{-3}, $s_v = 10.85$ m, $s_{inj} = 5$ m and various T_{i_0}. Results are shown in Figs. 11 and 12. As can be seen, Fig. 12, the DIVIMP data follows the SFT fairly well — at least when the correction for the variation of $kT_i\tau_s$ in the FFf integral, Eq. (16), is allowed for; this is a substantial correction here due to the large Δs. There is not a significant effect of collisionlessness here, compared with Fig. 8, since T_{i_0} is lower, ~35 eV in this figure, vs. ~100 eV in Fig. 8, and also because Δs is larger, making $\lambda_{mfp}/\Delta s$ smaller still. Evaluation of T_o^{th} using Eq. (30) for this case, $n_0 = 10^{19}$ m^{-3}, $\Delta s = 5.85$ m, gives $T_o^{th} = 50$ eV. At $T_{i_0} = 50$ eV the leakage is indeed seen to be substantial whether as defined by $\bar{n}_t/n_p$, which is $\simeq 0.1$, or ϕ_{leak}/ϕ_{in}, which is also about 0.1.

5. Discussion and Conclusions

The two principal objectives of the present paper can be summarized as follows:

(a) to derive simple analytic approximations which describe — for the case of leakage as ions — the situation when the "Neuhauser/Krasheninnikov Criterion," Sec. 3.2, |FF| > |FiG|, is satisfied, but leakage can nevertheless occur, i.e., to identify the "sufficiency" condition for divertor retention to supplement the "necessary" N/K Criterion.

(b) to test these simple predictions, first (Part I) by comparison with a constrained DIVIMP code, so as to directly test the predictions in the presence of such effects as partial collisionality, and then (in Part II), by comparison with an unconstrained DIVIMP to test for other real effects such as leakage partly via the neutral state.

Divertor leakage of impurities has therefore here been modelled at a first level of approximation: one-dimensional leakage as ions along the SOL. A number of other simplifying assumptions were made, for example, a frozen charge state for the impurities. For such a simplified system an analytic Simple Fluid Theory for divertor leakage could be constructed. It was found that leakage for a *strictly* one-dimensional system will generally be unphysically high, often extremely so. It is essential to include cross-field loss to the periphery of the SOL and Private Plasma to obtain a realistic result. This can be done, to a first approximation, in a simple way which still leaves the model as essentially one-dimensional.

The principal conclusions from the Simple Fluid Theory are:

1. The leakage flux out of the divertor tends to vary as $\exp(-T_i^2)$.
2. The threshold temperature T_o^{th} at which leakage flux becomes "significant" ($n_{s_v}/n_p > 0.1$), varies as $T_o^{th} \propto (n_e\, s_v)^{1/2}$, where s_v is the characteristic scale length of hydrogenic ionization.
3. For most cases of sputtering from the target, the value of T_o^{th} is so high, $\gtrsim$ 100 eV, that it appears unlikely that divertor leakage would occur by the one-dimensioanl ion-transport mechanism considered here.

4. For "deep injection" cases, where the impurities are ionized at some considerable distance from the plates, values of T_o^{th} can be lower, and in a more physically likely range. In this situation it appears likely that for high heat input to the tokamak, the temperature in the divertor could increase above the threshold value, causing the divertor to go from a non-leaking to a leaking state. This appears to correspond to at least some of the experimental divertor studies carried out with recycling gases [1-6].

The predictions of the Simple Fluid Theory were compared with results from the Monte Carlo impurity transport code DIVIMP, for a range of sample cases. For strongly collisional cases, agreement was close. For weakly collisional cases, the Simple Fluid Theory overestimates divertor leakage.

In Part II of this study, in preparation, the various simplifying assumptions employed in Part I will be relaxed to see if this alters the basic conclusions given above:

(a) full 2-D motion of the impurity ions will be allowed,

(b) the impurities will be followed from the point of initial release as a neutral, with both neutral and ion leakage paths followed,

(c) plasma backgrounds will include flow reversal,

(d) the impurity ions will be allowed to thermalize naturally and to change their charge state by ionization and recombination.

It is known, experimentally, that divertor plate material *can* end up in the core plasma [32] — particularly at low density. From the present study it is concluded that this is unlikely to be due to direct, 1-D ion transport from the near-target region. In the future studies the possibility that this leakage can be due to neutral transport, or to successive sputtering and re-deposition steps along the walls or to flow reversal will be evaluated.

Acknowledgement

The authors wish to thank Alex Chankin, Wojiech Fundamenski, Lorne Horton, Sergei Krasheninnikov, Bruce Lipschultz, Guy Matthews, Garry McCracken, Josef Neuhauser and C. S. Pitcher for most helpful discussions. This work was supported by the Canadian Fusion Fuels Technology Project.

Table II

Different Cases Used for DIVIMP Calculations

Case	T_{i_o} [eV]	dT_i/ds [eV/m]	n_e [m^{-3}]	$\bar{s}_{inj}$ [m]	s_v [m]	v_D [m/s]	E [V/m]
A	10	1.38 (constant)	10^{19}	0.15	1.2	Varied -875 to -1500	0
B	Varied 10 to 130 eV	From Eq. (26) with f_{cond}=0.1, M_D=0.1	10^{20}	0.15	1.2	-0.1 c_{s_o}	0
C	50	0	10^{18}, 10^{19}, 10^{20}	0.15	1.2	0	-25
D	10	0	10^{19}	0.15	1.2	-112.2	0
E	Varied 10 to 130 eV	From Eq. (26) with f_{cond}=1, M_D=1	10^{19}	0.15	1.2	-1 c_{s_o}	0
F	Varied 20 to 50 eV	From Eq. (26) with f_{cond}=1, M_D=0.1	10^{19}	5	10.85	-0.1 c_{s_o}	0

Appendix
Treatment of Collisionality

The Spitzer collision times, τ_S, $\tau_{||}$, Eqs. (39), (41), are actually for 3-D motion while here we ignore the coupling between parallel and perpendicular motion. The use of these expressions for τ_S, $\tau_{||}$ then encounters a small inconsistency associated with the finite value of m_D/m_I, which causes τ_S to differ from $\tau_{||}$ by a factor $(1 + m_D/m_I)$ when "T_I" $\rightarrow T_D$: here the value of T_I used in Eqs. (40) and (41) is calculated from:

$$\Delta T_I^f = (T_D - T_I^f)\, \Delta t/\tau_T \tag{A1}$$

where τ_T is the Spitzer energy transfer collision time:

$$\tau_T = \frac{m_I T_D (T_D/m_D)^{1/2}}{1.4\times10^5\, n_D Z_I^2\, \ell n\, \Lambda} \tag{A2}$$

where the same convenient units are used as for Eq. (39). The superscript "f" is for "formula", and is needed here to distinguish this from the value of T_I which can be directly extracted from the actual ion velocity distribution itself. We denote the latter by T_I^d; "d" for "distribution".

Ideally, of course, $T_I^f = T_I^d$. This will not happen, however, if the $(1 + m_D/m_I)$ term is present in τ_S, Eq. (39), but absent in $\tau_{||}$, Eq. (41). This is seen most simply for the situation where $T_I^f = T_D$: at each time step the ion velocity is incremented by $\Delta v = (kT_D/m_I)^{1/2}\, (2\Delta t/\tau_{||})^{1/2}\, r_G$, giving an average value of $\langle(\Delta v)^2\rangle = (2kT_D/m_I)\, (\Delta t/\tau_{||})\, \langle r_G^2\rangle = (2kT_D/m_I)\, (\Delta t/\tau_{||})$; thus the power input rate, $P_{in} = \frac{1}{2} m_I \langle(\Delta v)^2\rangle/\Delta t = kT_D/\tau_{||}$. For an individual ion with velocity v the energy loss rate is mv^2/τ_S and so for the velocity distribution varying as $\exp(-mv^2/2kT_I^d)$ the average power loss rate is readily shown to be $P_{out} = kT_I^d/\tau_S$. Setting $P_{in} = P_{out}$ gives $T_I^d/T_D = \tau_S/\tau_{||} = (1 + m_D/m_I)^{-1} = 0.857$ for carbon. Runs with these values of τ_S, $\tau_{||}$ in

DIVIMP, and with all forces turned off except friction and with $v_D = 0$, did indeed give a velocity distribution of C-ions with such a depressed temperature. While this discrepancy is of no practical consequence, it is potentially confusing. Rather than removing it by employing a full 3-D treatment of the ion collisions, a simple *ad hoc* 1-D approximation has been used here of re-defining $\tau_{||}$ to also have a factor $(1 + m_D/m_I)$ in the denominator. With this approximation, one then finds that $T_I^d = T_I^f$: Fig. 13 shows the velocity distribution for C^{4+} ions which were injected as 50 eV C^{4+} into a deuterium plasma with $T_D = 50$ eV, $n_e = 10^{19}$ m^{-3} constant in space; all forces off except friction with $v_D = 0$; the ions were injected very far from the target so as to give the distribution a chance to fully develop (average dwell time of ions in the plasma = 94 ms, to be compared with the Maxwellianization time, here $\approx\tau_{||} \approx 20$ μs). As can be seen, the ion velocity distribution follows the expected form $\exp(-mv^2/2kT_D)$ over about 4 orders of magnitude. When using the value of $\tau_{||}$ without the $(1 + m_D/m_I)$ factor, the velocity profile was found to obey an exponential form just as well, but the exponent corresponded to a temperature of 0.86 T_D.

It is not merely a matter of convenience to calculate T_I from T_I^f, Eq. (A1); this also side-steps the problem that often the velocity distribution does *not* follow an exponential form to the high precision shown in Fig. 13. Often the ions are not in a particular charge state long enough to fill out the distribution completely. Also, the background ion temperature is generally not constant in space and the impurity ions can move through changing temperature conditions before they have had a chance to fully fill out the distribution. Figure 14 shows the velocity distribution for C^+ to C^{4+} for injection (as C^+) into a constant plasma background of $T_e = T_D+ = 50$ eV, $n_e = 10^{19}$ m^{-3}. Injection was far from the targets so that true loss from the plasma was not a factor, ions were killed off, however, with characteristic time 1 ms. The ions were injected with an average energy of 1 eV. Figure 14 thus shows both the effects of heating-up, and of incomplete Maxwellianization. For this case:

State	$\tau_{\|\|}$ [μs]	τ_{iz} [μs]	T_I^f [eV]
C^+	17	5.5	2.8
C^{2+}	33	26	23
C^{3+}	31	150	47
C^{4+}	18	>1 ms	~50

The values of T_I^d, found by making straight line approximations to the curves in Fig. 4, correspond approximately to T_I^f.

The SFT assumes, of course, fully Maxwellian ions and so this is a further aspect of the real situation in a plasma which is tested for when using DIVIMP, i.e., this additional aspect of partial collisionality.

Earlier applications of DIVIMP and LIM employed *spatial*, rather than *velocity* (parallel) diffusion (say $\Delta t = \tau_{coll}$, then $\Delta v = \sqrt{2}\, r_G v_T$ with $v_T \equiv (kT_I/m_I)^{1/2}$, giving $\Delta s = \sqrt{2}\, r_G v_T \tau_{coll}$ and so the parallel (spatial) diffusion coefficient $D_{\|} \equiv (\Delta s)^2)/2\tau_{coll} = (kT_I/m_I)\, \tau_{coll}$; previously a similar expression $D_{\|} \equiv (4kT_I/\pi m_I)\, \tau_{\|}$ was used in DIVIMP for spatial diffusion). For the most part, results are little influenced by which assumption is made, however, as Shimizu and Takizuka have pointed out [33] there are cases where differences are important and therefore velocity diffusion is to be preferred, since the Spitzer derivations are for velocity diffusion. Also, with regard to the above point of testing for the effect of partially-Maxwellianized velocity distributions it is necessary to use this approach. Velocity diffusion is therefore used here.

6. References

1. J. Roth, K. Krieger, G. Fussmann, *Nuclear Fusion* 32 (1992) 1835.
2. G. Janeschitz, G. Fussmann, P. B. Kotze, et al, *Nuclear Fusion* 26 (1986) 1725.
3. G. Janeschitz, R. Gianella, H. J. Jaeckel, et al, *Controlled Fusion and Plasma Heating, Europhysics Conference Abstracts* 14B, Part III, p. 1365 (1990).
4. G. Janeschitz, N. Gottardi, H. Jaeckel, et al, *Controlled Fusion and Plasma Heating, Europhysics Conference Abstracts* 15C, Part III, p. 97 (1991).
5. J. Roth, G. Fussmann, G. Janeschitz, et al, *Controlled Fusion and Plasma Heating, Europhysics Conference Abstracts* 15C, Part III, p. 201 (1991).
6. G. M. McCracken, F. Bombarda, M. Graf, et al, *J. Nucl. Mater.* (1995).
7. P. C. Stangeby, J. D. Elder, *J. Nucl. Mater.* (1995).
8. P. C. Stangeby, J. D. Elder, D. Reiter, et al, *Contrib. Plasma Phys.* 34 (1994) 306.
9. J. Neuhauser, W. Schneider, R. Wunderlich, et al, *Nucl. Fusion* 24 (1984) 39.
10. S. I. Krasheninnikov, A. S. Kukushkin, T. K. Soboleva, *Nucl. Fusion* 31 (1991) 1455.
11. G. C. Vlases and R. Simonini, *Proc. 18th European Phys. Soc. Meeting*, Berlin (1991), Vol. 15C, Part III, p. 221.
12. G. Fussmann, *Divertor Retention for Noble Gases*, European Tokamak Workshop, Ising (1989).
13. P. C. Stangeby and J. D. Elder, *J. Nucl. Mater.* 196-198 (1992) 258.
14. P. C. Stangeby, C. Farrell, S. Hoskins, et al, *Nucl. Fusion* 28 (1988) 1945.
15. E. Cupini, A. DeMatteis, R. Simonini, *Monte Carlo Simulation of Neutral Particle Transport in Fusion Devices*, Rep. EUR XII 324/9, CEC, Brussels (1983).
16. P. J. Harbour and J. G. Morgan, Proc. 11th European Physics Society Meeting (1983), Aachen, Vol. 7D, Part II, p. 427.

17. D. B. Heifetz, in *Physics of Plasma-Wall Interactions in Controlled Fusion* (Proc. NATO Advanced Study Institute, Val-Morin, Quebec, 1984), NATO ASI Series, Vol. 131, Plenum Press, New York (1986) 695.

18. D. Reiter, *The EIRENE Code,* Version Jan. 1992, User Manual, KFA Jülich, Report JÜL-2599 (1992) and KFA Jülich Report JÜL-1947 (1984).

19. Yu. L. Igitkhanov, *Contrib. Plasma Phys.* 28 (1988) 477.

20. R. Zagorski, F. Romanelli, *Contrib. Plasma Phys.* 34 (1994) 331.

21. J. Neuhauser, W. Schneider, R. Wunderlich and K. Lackner, *J. Nucl. Mater.* 121 (1984) 194.

22. S. I. Krasheninnikov, private communication (1995).

23. B. Lehnert, *Nucl. Fusion* 23 (1983) 1327.

24. B. Lehnert, Plasma Phys. *Controll. Fusion* 26 (1984) 1237.

25. M. F. A. Harrison, P. J. Harbour, E. S. Hotston, et al, *Nucl. Fusion Technol.* 3 (1983) 432.

26. K. F. Alexander, K. Guenther, W. Hintze, et al, *Nucl. Fusion* 26 (1986) 1575.

27. W. Eckstein, C. Garcia-Rosales, J. Roth et al, *Sputtering Data,* IPP 9/82, Garching (1993).

28. J. Bohdansky (1984) Special Issue of Nucl. Fusion, p. 61.

29. L. Spitzer, *Physics of Fully Ionized Gases,* Interscience Publishers, New York, 2nd Edition (1962).

30. R. Simonini, A. Taroni, M. Keilhacker, et al, *J. Nucl. Mater.* 196-198 (1992) 369.

31. D. Reiter, *J. Nucl. Mater.* 196-198 (1992) 80.

32. J. Roth and G. Janeschitz, *Nucl. Fusion* 29 (1989) 915.

33. K. Shimizu and T. Takizuka, *Tech. Meeting on ITER Divertor Physics Design,* Feb. 1994, Garching.

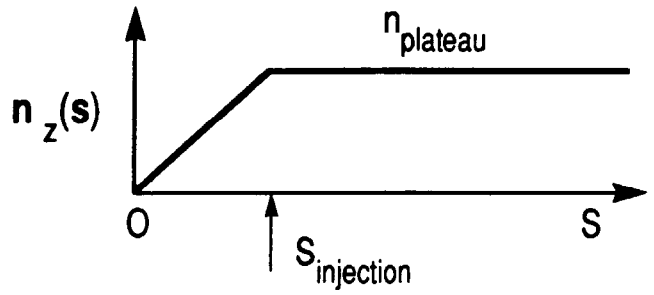

1. The impurity density profile along $\vec{B}$ for the case of (parallel) diffusion only.

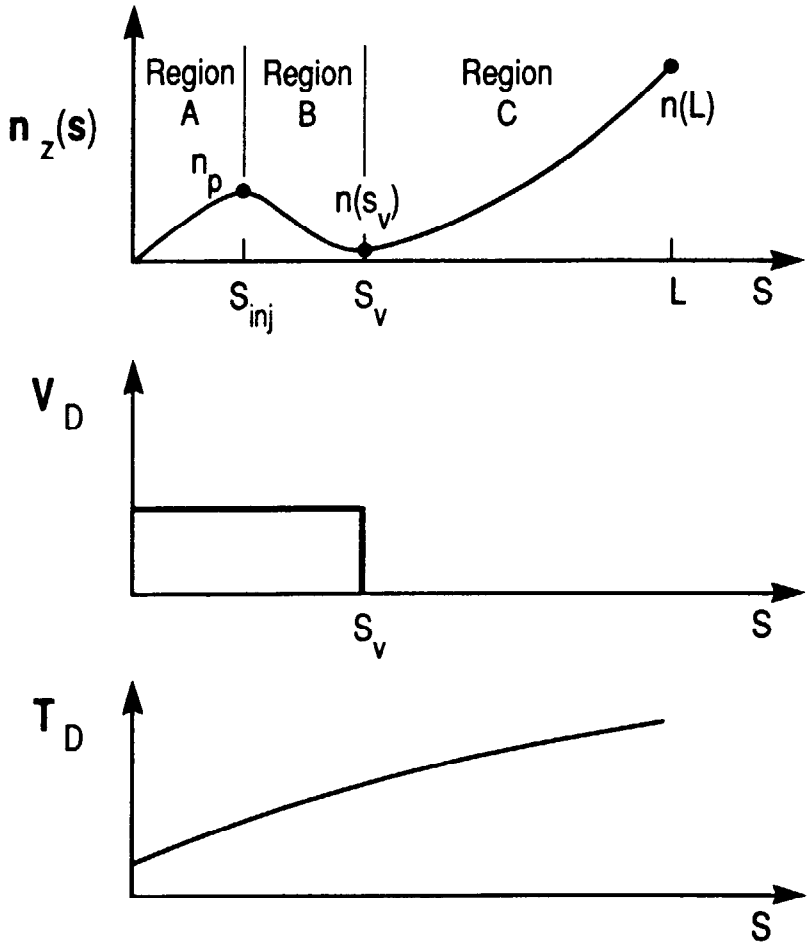

2. The general impurity density profile along $\vec{B}$ allowing for friction, temperature-gradient forces, parallel-diffusion, etc. See text, Section 3.

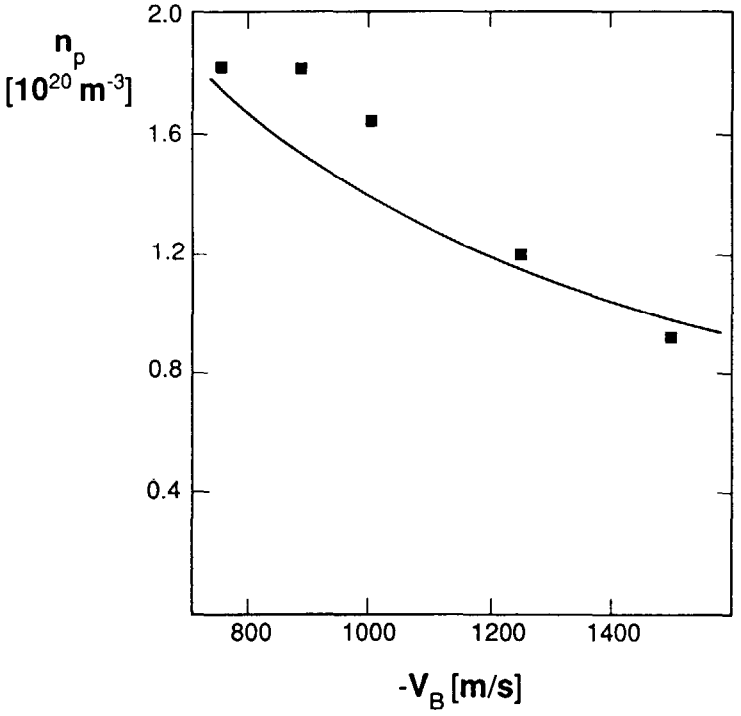

3. The impurity density peak value near the target n_p: Comparison of the value from the Simple Fluid Theory, solid line, and results (dots) from the DIVIMP code, for Case A conditions: $T_D(0)$ = 10 eV, dT_D/ds = 1.38 eV/m, $n_e = 10^{19}$ m^{-3}, $\bar{s}_{inj}$ = 0.15 m, s_v = 1.2 m, various values of the background deuterium velocity, $v_B \equiv v_D$. A highly collisional case, $\lambda_{mfp} \approx 1$ cm.

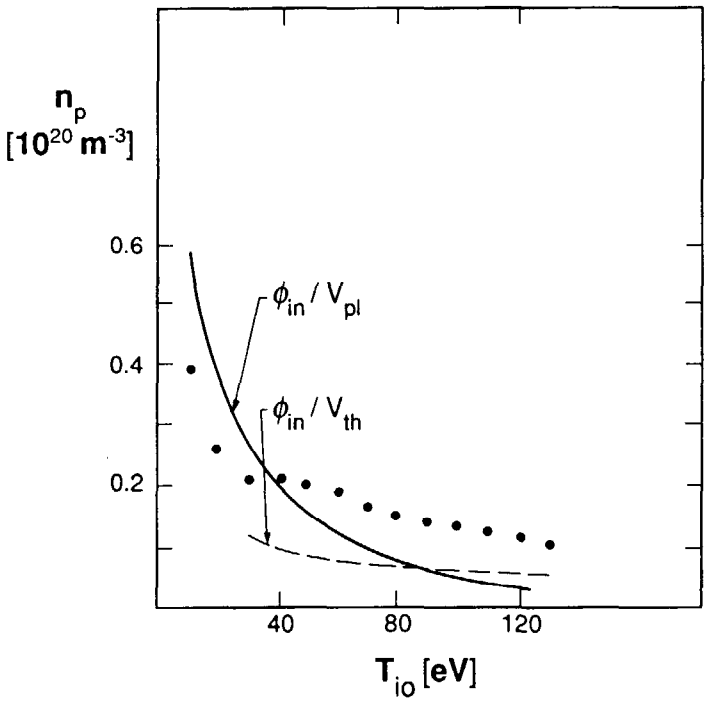

4. As Fig. 3 but for Case B conditions: $n_e = 10^{20}\ m^{-3}$, $\bar{s}_{inj} = 0.15$ m, $s_v = 1.2$ m, $M = 0.1$, $f_{cond} = 0.1$, temperature gradient given by Eq. (26), various values of $T_D(0) \equiv T_{i_o}$. Solid line from Simple Fluid Theory high collisionality assumption, $n_p = \phi_{in}/v_{pl}$; dashed line, simple collisionless assumption, $n_p = \phi_{in}/v_{th}$; points are DIVIMP results. For $T_{i_o} = 110$ eV, $\lambda_{mfp} \approx \bar{s}_{inj}$, thus one expects results to approach ϕ_{in}/v_{pl} for low T_{i_o}, and ϕ_{in}/v_{th} for high T_{i_o}, approximately as seen.

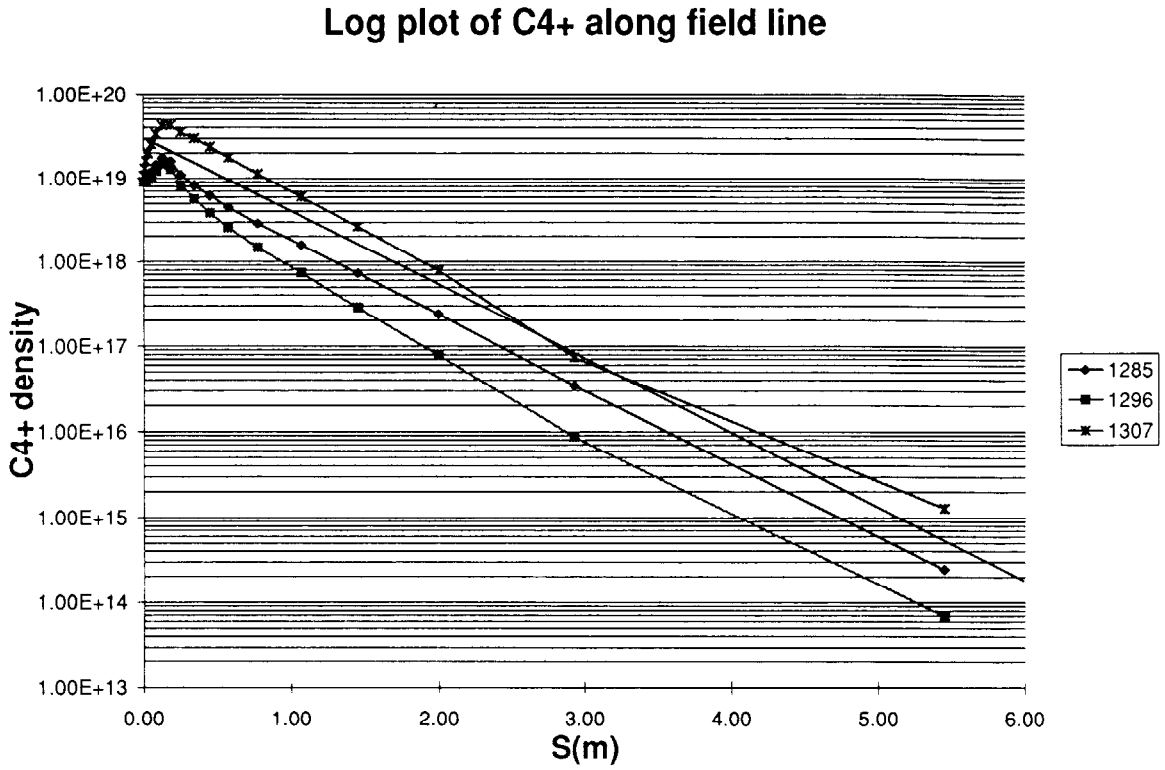

5. Density decay region. C^{4+} density profile, n(s) for the case with only the Electric Field on and no other forces (except parallel diffusion, i.e., the impurity pressure gradient force). Thus one expects n(s) to satisfy the Boltzmann Relation, which for the conditions assumed here, T_i = 50 eV, E = -25 V/m, corresponds to n(s) $\propto$ exp(-2s); the latter slope is shown as the line without points. DIVIMP results for various plasma densities: ■ 10^{18} m^{-3}, ◆ 10^{19} m^{-3}, ✶ 10^{20} m^{-3}, showing that the Boltzmann Relation is well-satisfied, independent of collisionality.

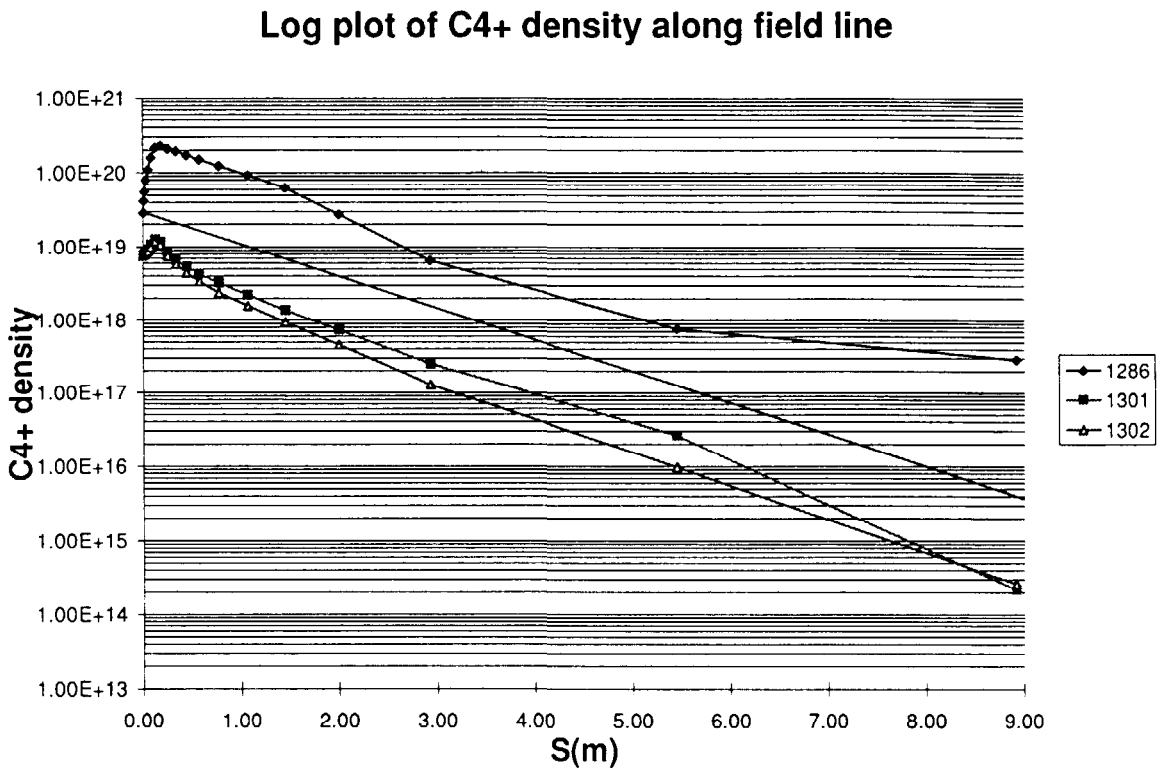

6. Density decay region. As for Fig. 5 but the only forces are friction due to D^+ flow at specified velocity, and parallel diffusion. DIVIMP results for various plasma densities, temperature and D^+ flow velocities:

(a) ◆ $n_e = 10^{19}$ m^{-3}, $T_D = 10$ eV, $v_D = 112$ m/s ($\therefore \lambda_{mfp} \approx 10^{-2}$ m)

(b) ■ $n_e = 10^{19}$ m^{-3}, $T_D = 100$ eV, $v_D = 3.55\times10^4$ m/s ($\therefore \lambda_{mfp} \approx 1$ m)

(c) ▲ $n_e = 10^{18}$ m^{-3}, $T_D = 100$ eV, $v_D = 3.55\times10^5$ m/s ($\therefore \lambda_{mfp} \approx 10$ m)

These plasma conditions were contrived to give the same value of $\lambda_{\|}^{SFT} \equiv D_{\|}/v_D = 1$ m here; such a slope is shown as the line without points. Clearly the SFT is approximately satisfied both for highly collisional and highly collisionless regimes for Region B, the density decay region.

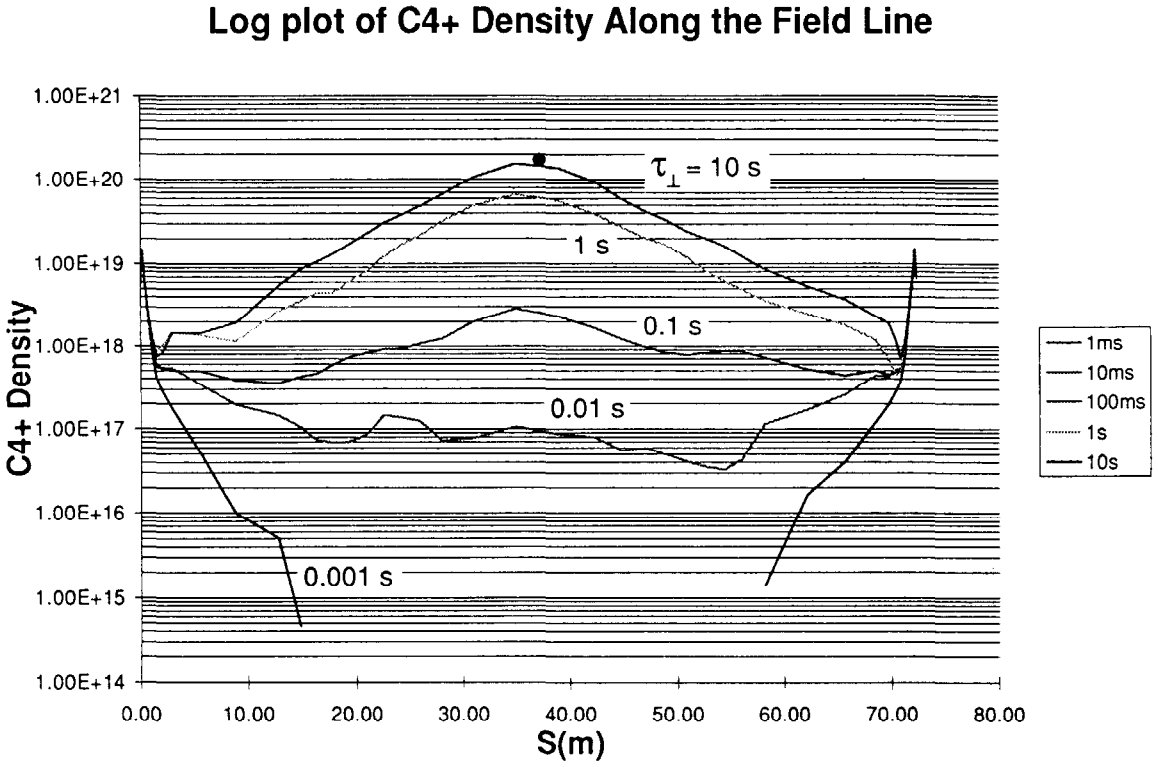

7. DIVIMP-calculated n(s) profiles of C^{4+} for Case B plasma conditions (see text), T_{i_o} = 100 eV, $\bar{s}_{inj}$ = 0.15 m, s_v = 1.2 m. Various values of $\tau_\perp$. The solid dot is calculated from SFT for $\tau_\perp = \infty$. Clearly divertor leakage is catastrophic unless $\tau_\perp \lesssim 100$ ms.

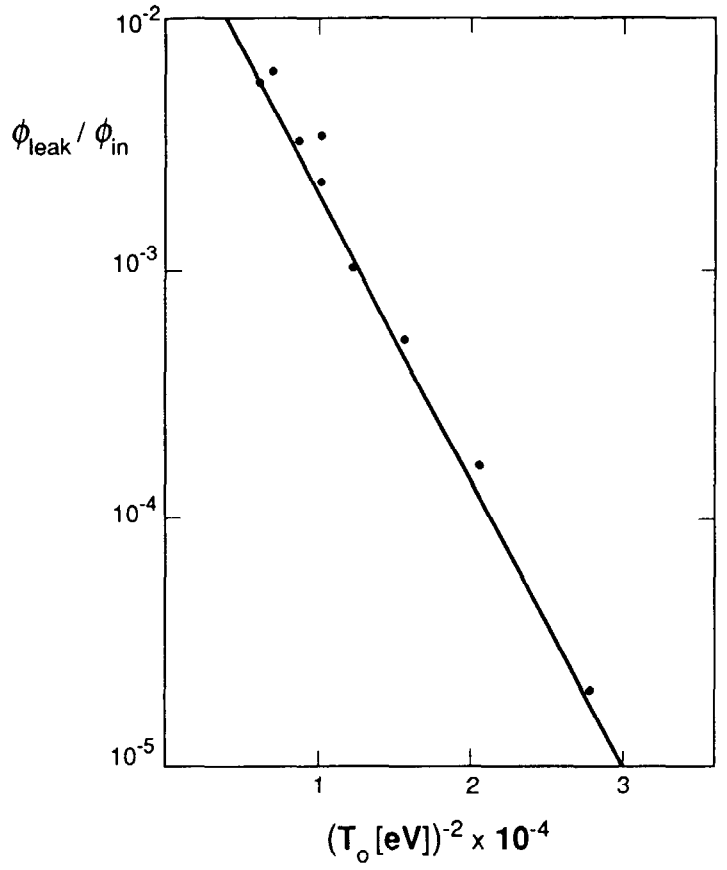

8. Points are DIVIMP-calculated ϕ_{leak}/ϕ_{in} for Case B, $n_e = 10^{20}$ m^{-3}, as a function of T_o. Highly collisional case, $\lambda_{mfp} \lesssim 0.1$ m. Solid line is from Simple Fluid Theory.

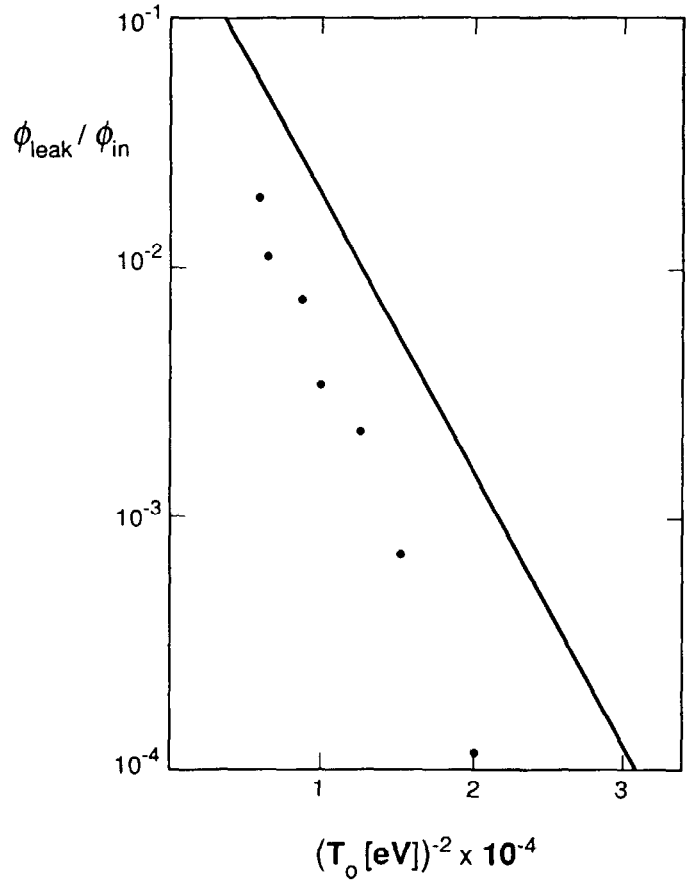

9. As Fig. 8 but for Case E, $n_e = 10^{19}$ m^{-3}. For this marginally-collisional case, where $\lambda_{mfp} \approx 1$ m, the agreement with the Simple Fluid Theory is less good. The SFT overestimates the leakage.

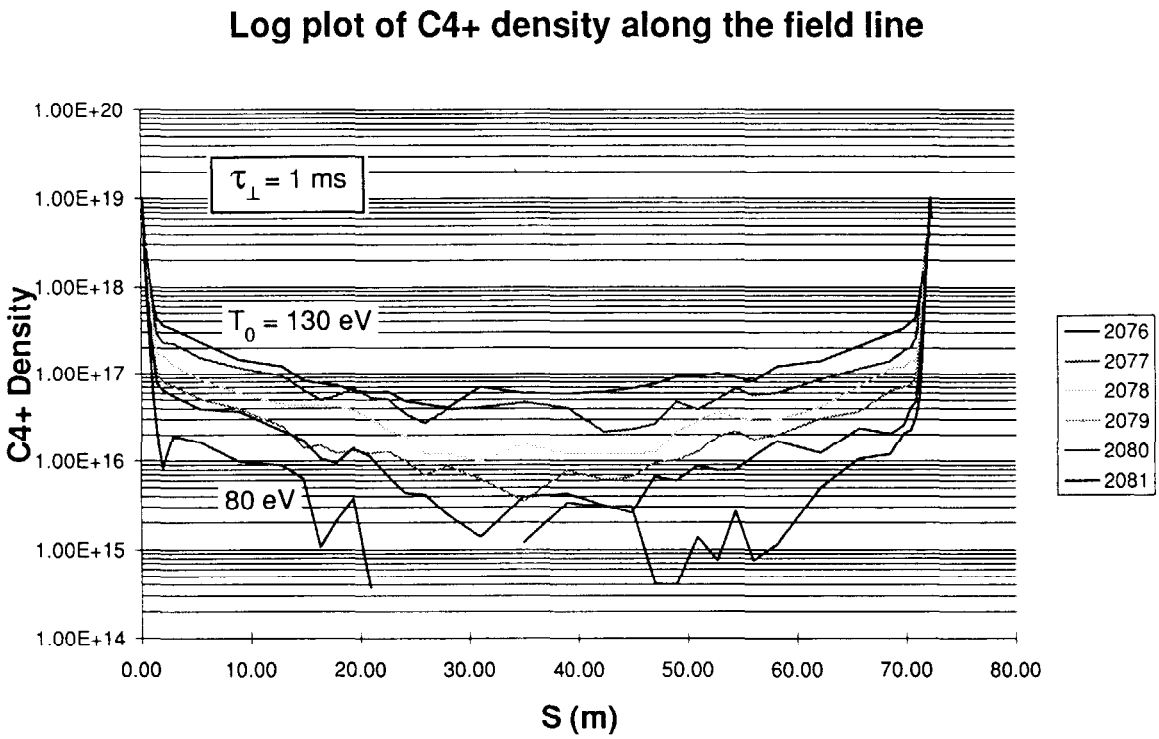

10a. DIVIMP-calculated n(s) (C^{4+}) profiles for Case E, $n_e = 10^{19}$ m^{-3}, $\tau_\perp = 1$ ms, various T_o: 80, 90, 100, 110, 120, 130 eV from bottom to top. Evidently for such a short $\tau_\perp$ divertor retention is excellent even at $T_o = 130$ eV.

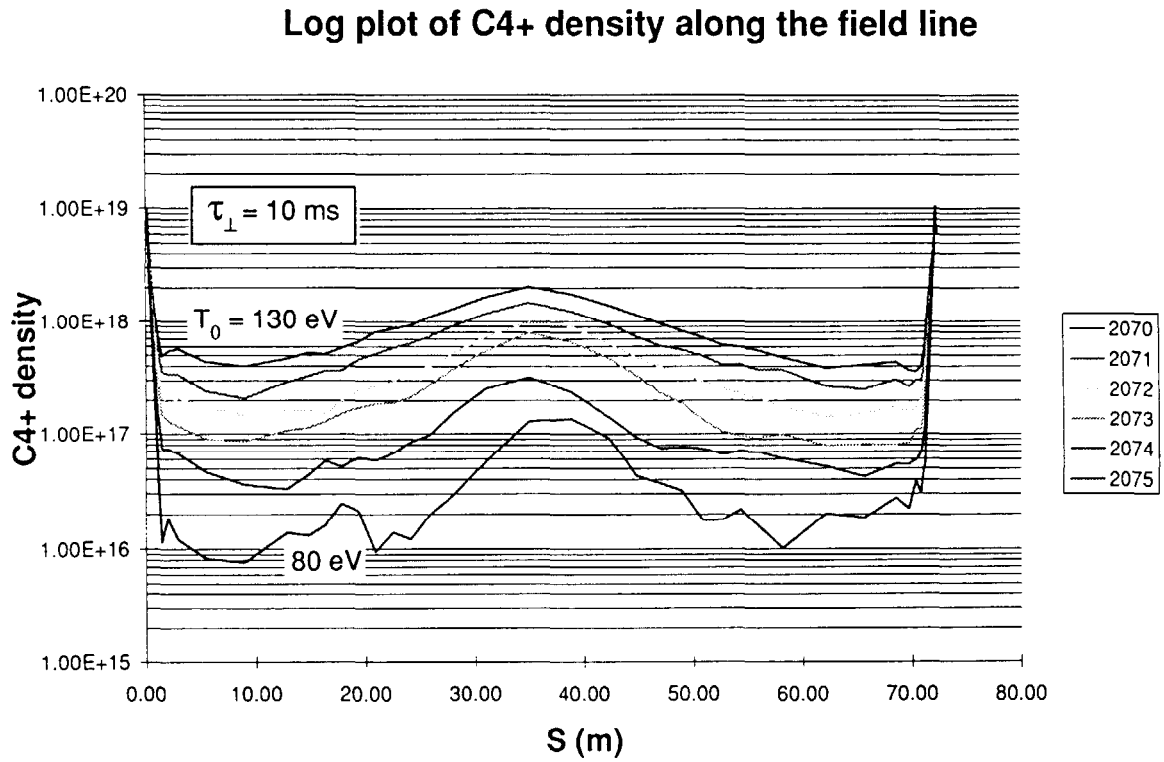

10b. As Fig. 10a but for $\tau_\perp = 10$ ms. Even for this longer — and possibly more realistic — $\tau_\perp$, divertor retention is good (i.e., $n_u/n_p \lesssim 0.1$) for $T_o < 110$ eV.

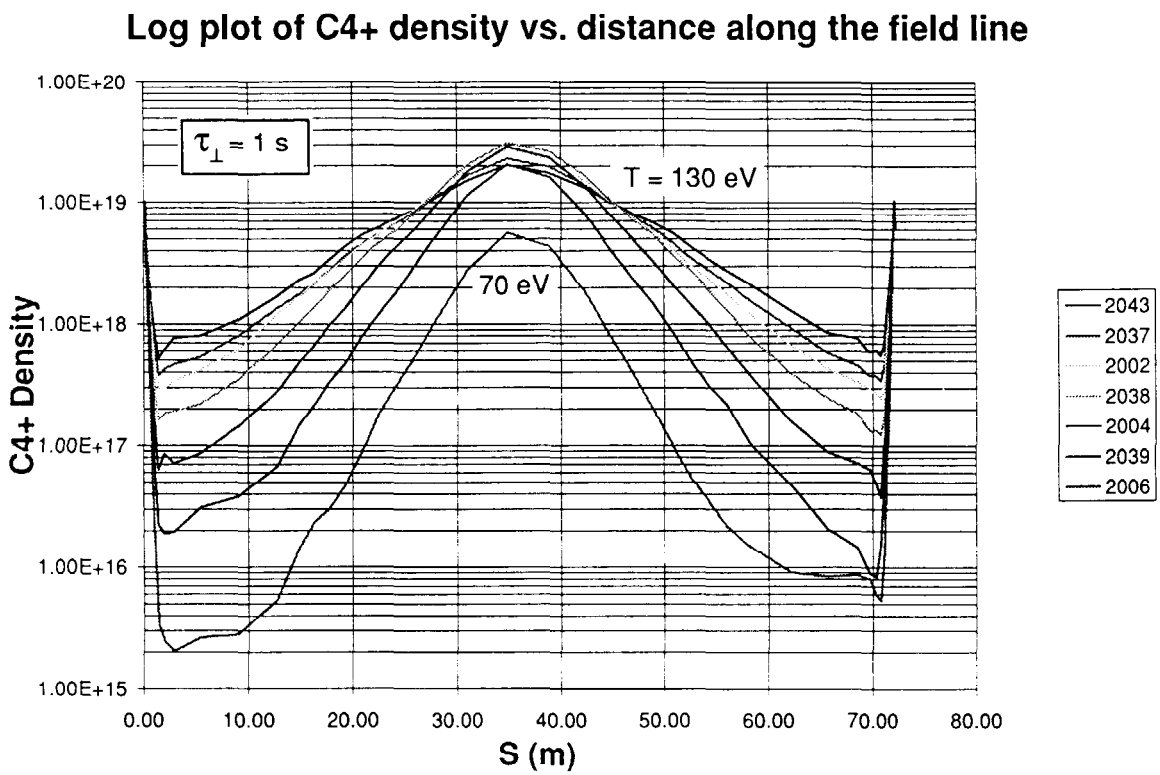

10c. As Fig. 10a but for $\tau_\perp = 1$ s. Lowest curve for 70 eV, highest for 130 eV, steps of 10 eV. For such unrealistically long $\tau_\perp$, divertor leakage is significant even for T_o as low as 70 eV.

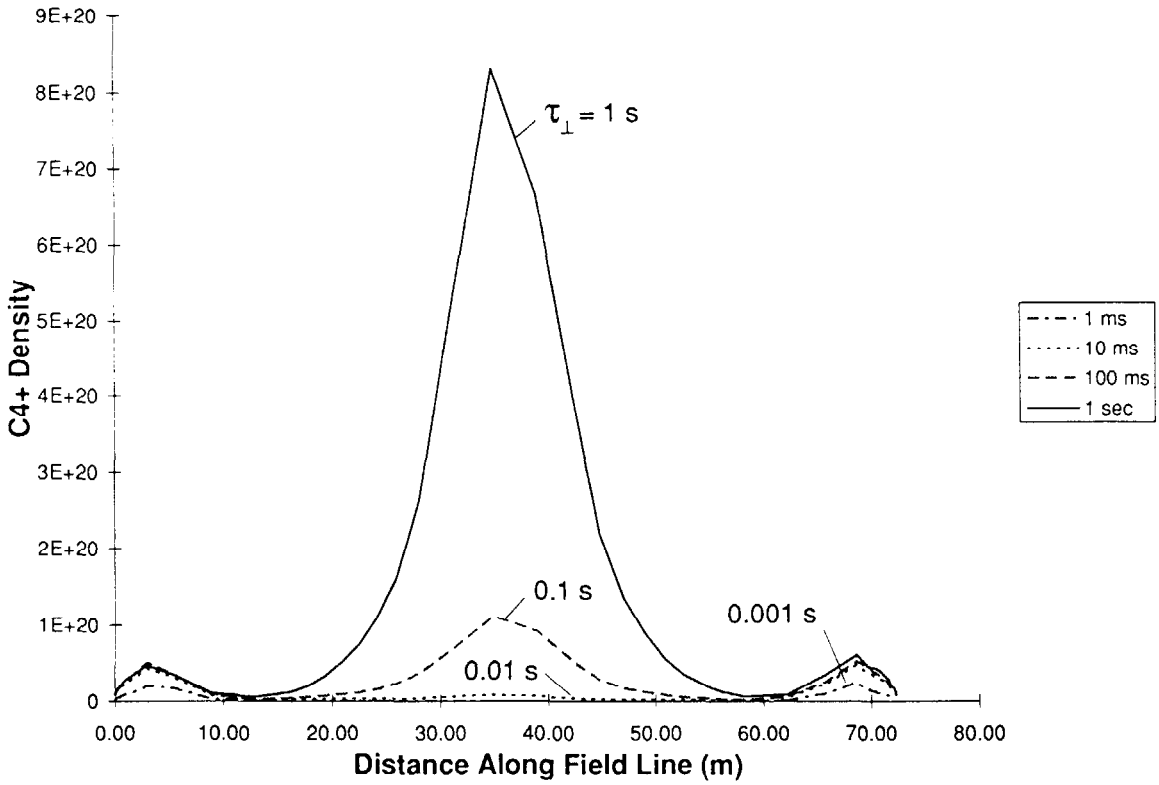

11. DIVIMP-calculated C^{4+} profiles for Case F, a "deep injection" case: $n_e = 10^{19}$ m^{-3}, $T_{i_o} = 50$ eV, $s_{inj} = 5$ m, $s_v = 10.85$ m, $M_D = 0.1$, $f_{cond} = 1$, various $\tau_\perp$. Evidently only for $\tau_\perp \lesssim 10$ ms is divertor retention acceptable for this value of T_{i_o}, and for these parameters.

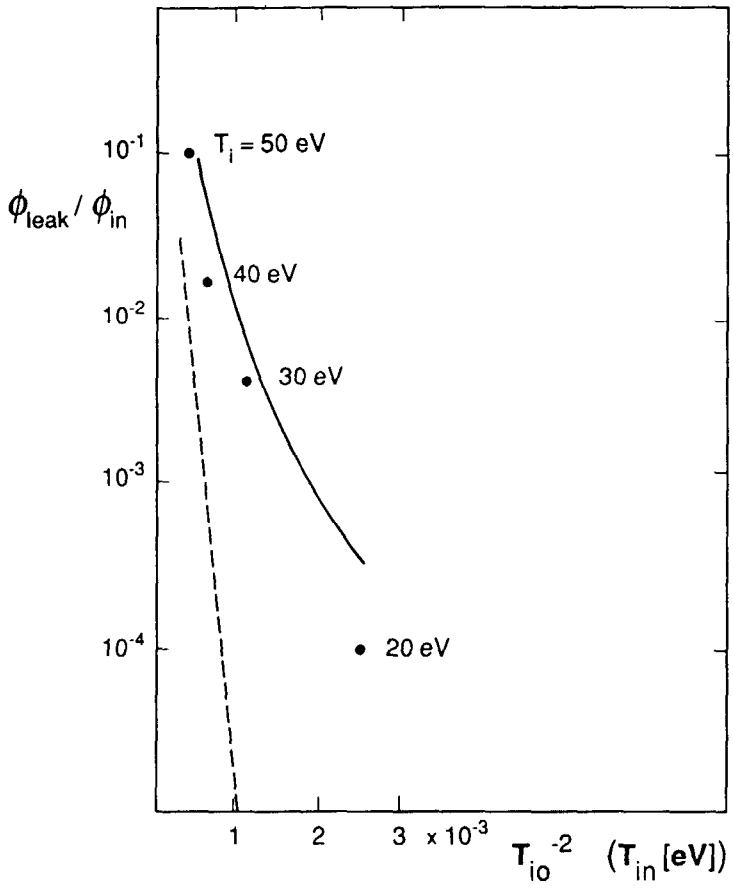

12. DIVIMP-calculated ϕ_{leak}/ϕ_{in} for Case F, "deep injection" case (points). Solid curve is for Simple Fluid Theory allowing for the spatial variation of $kT_i\tau_s$ in the friction force integral, Eq. (16); dashed line neglects that variation.

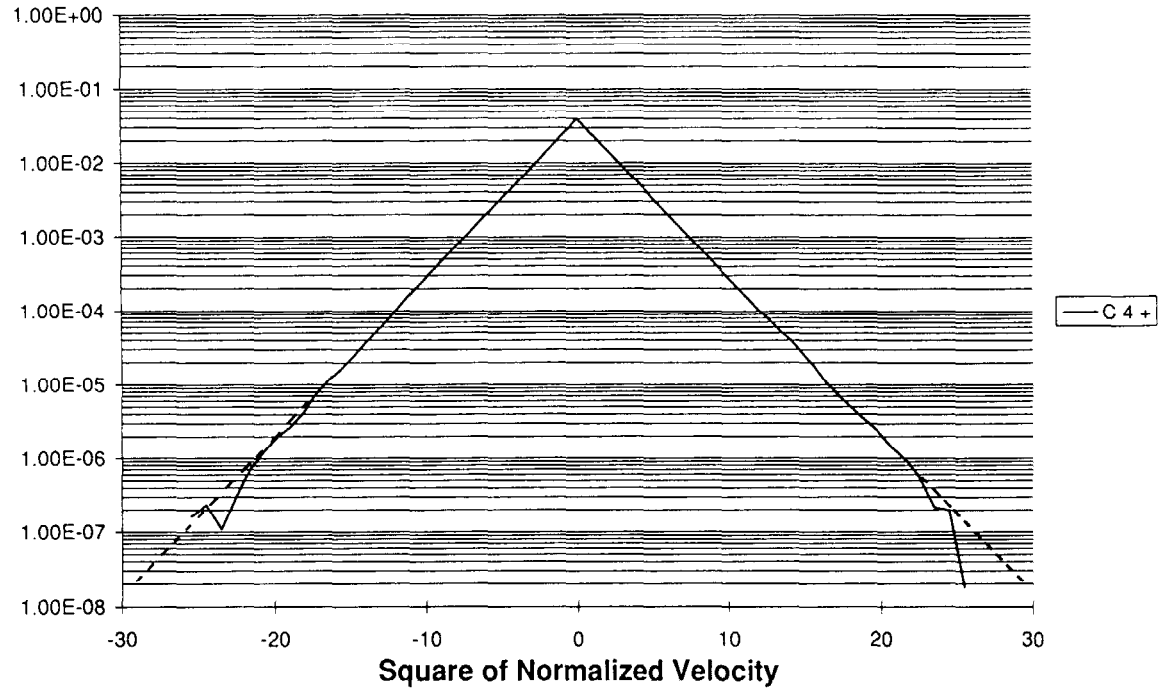

13. The DIVIMP-calculated velocity distribution for C^{4+} ions in a D^+/e plasma of $T_D = 50$ eV, $n_e = 10^{19}$ m^{-3} for a long dwell-time, ~100 ms; Maxwellianization time ≈20 μs. The horizontal scale is in units of (kT_D/m_C), thus if the carbon ions were fully thermalized to the D^+, their distribution would vary as $\exp(-m_C v^2/2kT_D)$, shown as dashed lines, which is seen to be the case over 4-5 orders of magnitude.

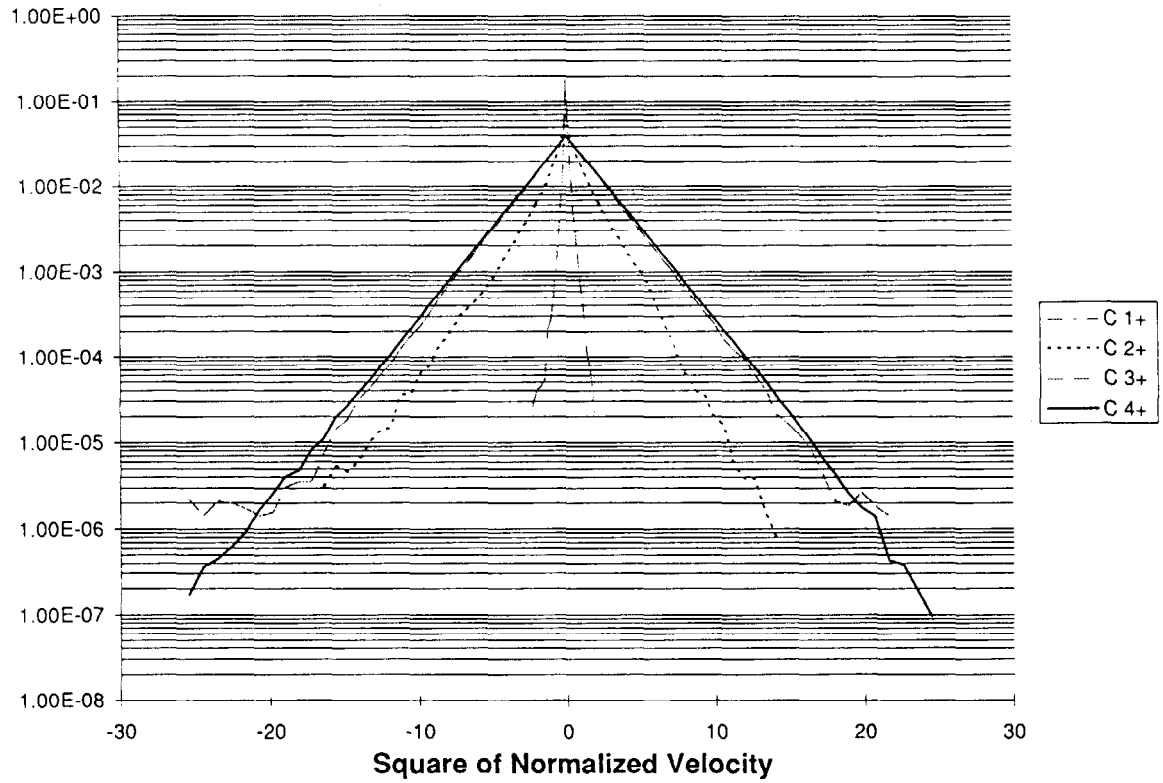

14. The same as Fig. 13 but for 1 eV C^+ ions injected into a plasma of $T_e = T_D = 50$ eV, $n_e = 10^{19}$ m^{-3} and allowed to thermalize and ionize. The finite thermalization of the lower charge states is evident. It is also clear that the lower charge states are less fully Maxwellianized — particularly the high energy tails.